

UNCLASSIFIED

AD 275 569

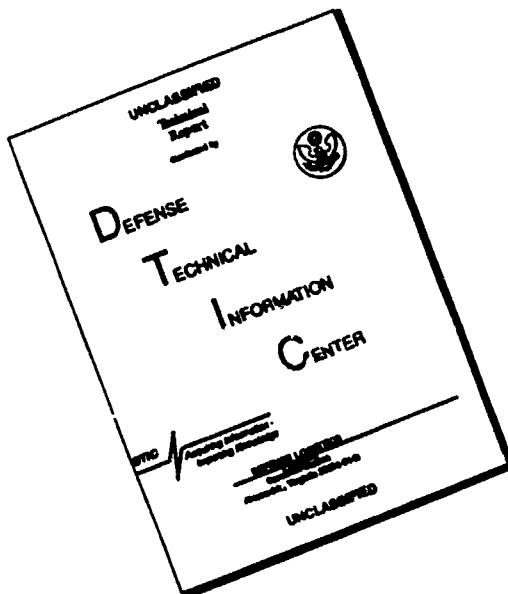
*Reproduced
by the*

**ARMED SERVICES TECHNICAL INFORMATION AGENCY
ARLINGTON HALL STATION
ARLINGTON 12, VIRGINIA**



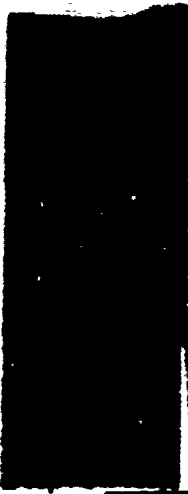
UNCLASSIFIED

DISCLAIMER NOTICE



THIS DOCUMENT IS BEST QUALITY AVAILABLE. THE COPY FURNISHED TO DTIC CONTAINED A SIGNIFICANT NUMBER OF PAGES WHICH DO NOT REPRODUCE LEGIBLY.

NOTICE: When government or other drawings, specifications or other data are used for any purpose other than in connection with a definitely related government procurement operation, the U. S. Government thereby incurs no responsibility, nor any obligation whatsoever; and the fact that the Government may have formulated, furnished, or in any way supplied the said drawings, specifications, or other data is not to be regarded by implication or otherwise as in any manner licensing the holder or any other person or corporation, or conveying any rights or permission to manufacture, use or sell any patented invention that may in any way be related thereto.



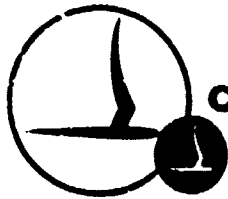
275 569

**CATALOGED BY ASTIA
AS AD NO. _____**

**FIRST INTERIM REPORT ON THE
HYDRODYNAMICS AND STABILITY AND CONTROL OF A
TANDEM PROPELLER SUBMARINE**

**Prepared For
Office of Naval Research
Department of the Navy
Washington 25, D.C.**

**By: F. Dell'Amico and L. Segel
Contract Nonr-3659(00) (FBM)
CAL Report No. AG-1634-V-1
26 March 1962**



CORNELL AERONAUTICAL LABORATORY, INC.
OF CORNELL UNIVERSITY, BUFFALO 21, N. Y.

CORNELL AERONAUTICAL LABORATORY, INC.
of Cornell University
Buffalo, New York

**FIRST INTERIM REPORT
ON THE
HYDRODYNAMICS AND STABILITY AND CONTROL
OF A
TANDEM PROPELLER SUBMARINE**

Contract Nonr-3659(00) (F&M)

CAL Report No. AG-1634-V-1

26 March 1962

**Prepared For
Office of Naval Research
Department of the Navy
Washington 25, D. C.**

by
**F. Dell'Amico and L. Segel
Vehicle Dynamics Department**

FOREWORD

This report describes the work performed by the Cornell Aeronautical Laboratory under Contract Nonr-3659(00) (FBM), sponsored by the Office of Naval Research of the Department of the Navy. The time-period covered is from 16 October 1961 to 25 March 1962. The program is being conducted under the general direction of Cdr. F. R. Haselton, Code 466, and R. Cooper, Code 438, of the Office of Naval Research.

The authors wish to express their gratitude to Mr. D. C. Clark of the Vehicle Dynamics Department of CAL, for his contributions to the stability and control studies, and to Messrs. G. Tufts, E. Sullivan, and F. DuWaldt, of the Applied Mechanics Department of CAL, for performing the theoretical hydrodynamics studies and for valuable contributions to the entire program.

ABSTRACT

Hydrodynamic and stability and control characteristics are investigated for a novel submarine configuration employing tandem, large hub-to-diameter ratio propellers whose blades are pitched collectively and cyclicly. Stability coefficients for the hull and the propeller are derived. Expressions for the control forces and moments generated by the propellers are developed and the perturbation equations of motion are used to analyze the controlled dynamics of the submarine. An analysis of the motions in the vertical plane indicates that the submarine can be stabilized at high speeds by automatic control of collective and cyclic pitch and that reasonable maneuverability can be obtained.

TABLE OF CONTENTS

	<u>Page No.</u>
FOREWORD	i
ABSTRACT	ii
TABLE OF CONTENTS	iii
LIST OF FIGURES	iv
LIST OF TABLES	v
I. INTRODUCTION	1
II. STATUS OF PROGRAM AND SUMMARY OF CONCLUSIONS	3
2.1 Status of Program	3
2.2 Summary of Conclusions	4
III. SYMBOLS AND NOMENCLATURE	6
3.1 Nomenclature	6
3.2 Symbols	7
IV. POSTULATED TPS CONFIGURATION	13
4.1 Hull	13
4.2 Propellers	15
V. HYDRODYNAMIC ANALYSIS	18
5.1 General Remarks	18
5.2 Stability Coefficients of the TPS	21
5.3 Control Coefficients of the TPS	41
5.4 Added-Mass Coefficients	51
VI. EQUILIBRIUM EQUATIONS AND NUMERICAL DATA	52
6.1 Six-Degree-of-Freedom Equations of Motion	52
6.2 Trim Conditions - Two Propellers Operating	53
6.3 Trim Conditions - One Propeller Operating	55
6.4 Numerical Data	60
VII. STABILITY AND CONTROL STUDIES	66
7.1 General Remarks	66
7.2 The Linearized Equations of Motion	68
7.3 Analytical Studies	70
7.4 Stability Augmentation	71
7.5 Pitch-Plane Dynamics	73
7.6 Yaw-Plane Dynamics	87
VIII. REMAINING STUDIES	88
IX. REFERENCES	89
APPENDIX - The Linearized, Low-Speed, Hydrodynamic Forces and Moments Arising from the Propellers of the TPS	91

LIST OF FIGURES

<u>Fig. No.</u>		<u>Page No.</u>
4-1	Tandem Propeller Submarine	14
4-2	Propeller Sign Conventions	17
6-1	Single Propeller Trim Balance Conditions	58
6-2	Normalized Power Required for Single Propeller Trim Balance Conditions	59
7-1	Basic Submarine Response (All Feedback Gains Zero) Linear System	76
7-2	Decoupling Feedback - Linear (Unstable Pitch Response)	77
7-3	Decoupling Plus Direct-Axis Stabilization - Linear System	79
7-4	Direct-Axis Stabilization (No Control Coupling) - Linear	80
7-5	Direct-Axis Stabilization - Linear	81
7-6	Direct-Axis Stabilization - Nonlinear	82
7-7	Direct-Axis Stabilization - Linear	83
7-8	Decoupling + Direct-Axis Stabilization - Linear	85
7-9	Direct-Axis Stabilization	86

LIST OF TABLES

<u>Table No.</u>		<u>Page No.</u>
5-1	Tabulation of Nondimensional Hull Derivatives (TPS and Albacore)	23
5-2	Tabulation of Propeller Derivatives (One Propeller)	28
6-1	Physical Data	61
6-2	Total Hull and Propeller Derivatives	63
6-3	Primary Control Coefficients	65
6-4	Control Coupling Coefficients	65

I

INTRODUCTION

In October 1961 the Cornell Aeronautical Laboratory, Inc. undertook to investigate the hydrodynamic and stability and control aspects of a novel submarine configuration utilizing variable-pitch large hub-to-diameter-ratio propellers. The configuration, invented by Cdr. F. R. Haselton of the Office of Naval Research, employs two propellers mounted circumferentially (forward and aft) on a neutrally buoyant body of revolution, to produce any combination of forces and moments. By means of this arrangement, which has been called a Tandem Propeller Submarine (TPS), it is possible to produce control forces in all three degrees of freedom, or control moments in all three degrees of freedom, as well as combinations of forces and moments.

The work undertaken by the Cornell Aeronautical Laboratory has as its basic objectives (a) the theoretical determination of the hydrodynamic characteristics of the tandem propeller configuration, (b) an investigation of the trim and stability and control characteristics of the controlled submarine, and (c) a comparison between the TPS and a conventional submarine with respect to stability and control characteristics and handling qualities.

The work accomplished to date includes the following:

- (1) The hydrodynamics have been defined in terms of hull and propeller stability derivatives for the high-speed case (about 24 knots). Work on the hovering case is in progress.
- (2) The equations of motion for the high-speed case have been written and numerical values for all of the physical and hydrodynamic properties have been computed for the postulated submarine configuration.
- (3) The high-speed trim characteristics have been investigated for operation with one propeller and operation with two propellers.
- (4) The propulsion and control coefficients defining the generation of forces and moments as a function of collective and cyclic pitch control inputs have been determined for the high-speed case.
- (5) An analog-computer study of the pitch plane dynamics of the controlled (i. e. stability augmented) submarine has been performed for the high-speed case. The effects of pitch maneuvers on roll angle and forward speed, as well as the effects of certain nonlinear control coupling forces and moments on pitch dynamics have been determined.
- (6) Tentative control system gains for pitch attitude and depth-keeping loops have been selected. Two types of stabilization have been investigated and their differences noted for the pitch maneuvering mode of operation.
- (7) A limited analytical study of the yaw plane dynamics has been accomplished.

II

STATUS OF PROGRAM & SUMMARY OF CONCLUSIONS

2.1 STATUS OF PROGRAM

- (1) High-speed hydrodynamics are defined for the TPS configuration, permitting a high-speed stability and control investigation to ascertain the central issue of feasibility, namely: is sufficient cyclic pitch available to stabilize and provide maneuver control?
- (2) Low-speed (or hovering) hydrodynamics are tentatively defined for both the propeller and hull contributions. Calculations must be performed to assess:
 - (a) The relative contributions of the tandem propellers and the hull to the total hydrodynamic forces and moments acting on the TPS.
 - (b) The degree to which the propeller forces are simultaneously influenced by combined blade-pitch changes and changes in blade flight path-angle due to the motions of the submarine.

- (3) Equilibrium trim studies have been made to ascertain the ability to trim the TPS in steady longitudinal flight when one propeller only is used for propulsion.

2.2 SUMMARY OF CONCLUSIONS

- (1) Analysis of the stability coefficients for the high-speed case shows that, in comparison with conventional submarines, the gains in control effectiveness achieved at low and zero speeds (plus the gain in control flexibility) are obtained at a sacrifice of high-speed control effectiveness.
- (2) The TPS is dynamically unstable in pitch, unless control forces and moments are applied to modify and eliminate this instability. The instability arises primarily from the large unstable pitching moment due to angle-of-attack (M_w) relative to the levels of damping in pitch (M_g) possessed by the TPS.
- (3) The divergence in pitch motion, due to instability, is sufficiently severe to require automatic stabilization in contrast to manual stabilization.
- (4) Although other types of stabilizing feedbacks were investigated for use in an automatic pitch-control system, simple pitch-rate and pitch-angle feedbacks were found to be effective. Well-damped pitch-angle responses to pitching moment control inputs can be obtained in about 60 seconds. Corresponding steady-state dive or climb rates of about 6 ft/sec. are easily achieved. These figures do not represent maximum achievable performance.

- (5) An analog computer investigation shows that the level of the command control inputs must be limited to keep the propeller blade angles-of-attack within their stall limits when cyclic and collective pitch are used for automatic stabilization. Computed feedback-loop gains that originally appeared to be so large that continual saturation of the cyclic-pitch control would result, were found to be acceptable, provided limits were placed on maneuver demands.
- (6) Although an investigation of the yaw-plane dynamics has not been completed it is probable that conclusions, similar to those given above for pitch, will eventually be reached.
- (7) It has been shown that within certain speed limits it is possible to trim the TPS in high-speed, straight and level flight, with one propeller fixed and one operating. Speeds of about 15 knots can be achieved with a single propeller operating at 50 rpm. (An investigation of the problem of maneuvering the TPS with one propeller operating remains to be completed. It is anticipated that this control mode will present a serious problem.)
- (8) With respect to the overall stability and control problems, the tentative conclusion is reached that automatic control of the TPS submarine is feasible. Comparison with a conventional submarine has not yet been made nor has the question of handling qualities been examined fully.

III

SYMBOLS AND NOMENCLATURE

3.1 NOMENCLATURE

Forces and moments acting on the Tandem Propeller Submarine (TPS) are written in body axes. The $x-y-z$ body axis system is a right-handed orthogonal triad with its origin at the submarine center-of-gravity. x is positive forward, y is positive to starboard and z is positive down. Components of total linear and angular velocity along and around $x-y-z$ are u, v, w and p, q, r respectively. Generalized forces and moments are $X - Y - Z$ and $K - M - N$ along and around $x-y-z$.

Trim conditions will be denoted by a zero subscript and properties related to forward and aft propellers will be distinguished by subscripts f and a . Perturbations from trim in velocity are denoted by barred quantities, thus:

$$u = u_0 + \bar{u}, \quad v = v_0 + \bar{v}, \quad w = w_0 + \bar{w} \quad (1)$$

Angular velocity perturbations are defined by:

$$p = p_0 + \dot{\phi}, \quad q = q_0 + \dot{\theta}, \quad r = r_0 + \dot{\psi} \quad (2)$$

where ϕ, θ and ψ are the linearized (small-angle) Euler angles.

Stability derivatives will be identified by subscripts which indicate the perturbed variable. For example, $X_{\dot{u}}$ is an u -force derivative or coefficient denoting a change in u -force due to the u -velocity perturbation \dot{u} .

Other symbols, assumptions, etc. will be presented as they occur in the text. In addition, Section 3.2 contains a list of all of the symbols used in this report.

3.2 SYMBOLS

All symbols used in this report are listed below. Where used, the subscripts f and a denote forward and aft conditions.

Hull Characteristics

	<u>Units</u>
d = Max. hull diameter	ft
f = Fineness ratio = l/d	dimensionless
l = Length of submarine	ft
l_1 = Distance, fore point to c. g.	ft
l_2 = Distance, prop. plane to c. g. (l_2 carries no sign)	ft
z_0 = Metacentric height	ft
Δ = Submerged displacement (= Weight)	lbs

Propeller Characteristics

R = Average radius	ft
D = Average diameter	ft
N = Number of blades	
A = Blade area	ft ²
Ω = Blade angular velocity (Ω carries no sign)	rad/sec
n = Blade angular velocity (n carries no sign)	rev/sec

	<u>Units</u>
C_{L_2} :	Lift coefficient
C_{D_0} :	Profile drag coefficient
f_i :	Induced drag coefficient
γ :	Flight path angle of the blade (see Fig. 4-2) rad
α :	Blade angle-of-attack (see Fig. 4-2) rad
δ :	Total instantaneous blade pitch (see Fig. 4-2) rad
δ_0 :	Collective pitch (see Fig. 4-2) rad
$\Delta\delta$:	Change in collective pitch (see Fig. 4-2) rad
b_0 :	Blade angle of attack due to collective pitch ($b_0 = \delta_0 + \Delta\delta - \gamma_0$) rad
σ :	Blade azimuth angle in plane of prop (see Fig. 4-2) rad
$\delta_1 \sin \sigma$:	Sine component of cyclic pitch (see Fig. 4-2) rad
$\delta_2 \cos \sigma$:	Cosine component of cyclic pitch (see Fig. 4-2) rad

Kinematics

U :	Total velocity of c. g. ($U^2 = u^2 + v^2 + w^2$) ft/sec
u :	x -component of velocity (perturbation = \bar{u}) ft/sec
v :	y -component of velocity (perturbation = \bar{v}) ft/sec
w :	z -component of velocity (perturbation = \bar{w}) ft/sec
p :	x -component of total angular velocity (perturbation = \bar{p}) rad/sec
q :	y -component of total angular velocity (perturbation = \bar{q}) rad/sec
r :	z -component of total angular velocity (perturbation = \bar{r}) rad/sec
V :	Blade velocity relative to water (see Fig. 4-2) ft/sec

Mass/Inertia PropertiesUnits

$K_1 - K_2 - K_3 =$	Coefficients of accession to mass along $x - y - z$	dimensionless
$K_4 - K_5 - K_6 =$	Coefficient of accession to inertia around $x - y - z$	dimensionless
$m =$	Mass of submarine	#-sec ² /ft
$m_1 =$	Virtual mass along $x = m(1 + K_1)$	#-sec ² /ft
$m_2 =$	Virtual mass along $y = m(1 + K_2)$	#-sec ² /ft
$m_3 =$	Virtual mass along $z = m(1 + K_3)$	#-sec ² /ft
$I_{x_0} - I_{y_0} - I_{z_0} =$	Submerged moments of inertia about $x - y - z$	#-ft-sec ²
$I_{xx} =$	Virtual moment of inertia about $x = I_{x_0}(1 + K_4)$	#-ft-sec ²
$I_{yy} =$	Virtual moment of inertia about $y = I_{y_0}(1 + K_5)$	#-ft-sec ²
$I_{zz} =$	Virtual moment of inertia about $z = I_{z_0}(1 + K_6)$	#-ft-sec ²
$H =$	Propeller angular momentum	#-ft-sec
$\rho =$	Water density	#-sec ² /ft ⁴

Forces and Moments

$F_{x_0} =$	Trim thrust available from propeller(s)	#
$M_{x_0} =$	Trim moment at the propeller(s)	ft-#
$P_0 =$	Trim propeller(s) power	hp
$M_\theta =$	Metacentric pitching moment coefficient $= -m g z_0$	ft-#/rad
$X_C - Y_C - Z_C =$	Control (propeller) forces	#
$K_C - M_C - N_C =$	Control (propeller) moments	# ft

$\Sigma X - \Sigma Y - \Sigma Z =$	Combined propeller and hull hydrodynamic and hydrostatic forces	<u>Unit</u> #
$\Sigma K - \Sigma M - \Sigma N =$	Combined propeller and hull hydrodynamic and hydrostatic moments	#-ft

Hull Derivatives

X'_{u}	=	Dimensionless	x -force derivative due to \bar{u}
Y'_{v}	=	Dimensionless	y -force derivative due to \bar{v}
$Y'_{\dot{v}}$	=	Dimensionless	y -force derivative due to $\dot{\bar{v}}$
$Y'_{\dot{\phi}}$	=	Dimensionless	y -force derivative due to $\dot{\bar{\phi}}$
Z'_{w}	=	Dimensionless	z -force derivative due to \bar{w}
$Z'_{\dot{w}}$	=	Dimensionless	z -force derivative due to $\dot{\bar{w}}$
K'_{v}	=	Dimensionless	x -moment derivative due to \bar{v}
$K'_{\dot{\phi}}$	=	Dimensionless	x -moment derivative due to $\dot{\bar{\phi}}$
$K'_{\dot{v}}$	=	Dimensionless	x -moment derivative due to $\dot{\bar{v}}$
M'_{w}	=	Dimensionless	y -moment derivative due to \bar{w}
$M'_{\dot{w}}$	=	Dimensionless	y -moment derivative due to $\dot{\bar{w}}$
N'_{v}	=	Dimensionless	z -moment derivative due to \bar{v}
$N'_{\dot{v}}$	=	Dimensionless	z -moment derivative due to $\dot{\bar{v}}$
$N'_{\dot{\phi}}$	=	Dimensionless	z -moment derivative due to $\dot{\bar{\phi}}$

Propeller Terminology

X_{u}^p	=	Dimensional	x -force derivative due to \bar{u}_p^*	#/ft per sec
$X_{\dot{\phi}}^p$	=	Dimensional	x -force derivative due to $\dot{\bar{\phi}}_p$	#/rad per sec
Y_{v}^p	=	Dimensional	y -force derivative due to \bar{v}_p	#/ft per sec

* The p subscript denotes perturbations with respect to propeller axes. Propeller axes are parallel to body axes but with origin at $x = l_p$, forward and aft.

		<u>Unit</u>
Y_q^P	Dimensional y -force derivative due to $\dot{\Theta}_p$	#/rad per sec
$Z_{\dot{w}}^P$	Dimensional z -force derivative due to \dot{w}_p	#/ft per sec
$Z_{\dot{r}}^P$	Dimensional z -force derivative due to $\dot{\psi}_p$	#/rad per sec
$K_{\dot{p}}^P$	Dimensional x -moment derivative due to $\dot{\phi}_p$	#-ft/rad per sec
$K_{\dot{u}}^P$	Dimensional x -moment derivative due to \dot{u}_p	#-ft/ft per sec
$M_{\dot{q}}^P$	Dimensional y -moment derivative due to $\dot{\Theta}_p$	#-ft/rad per sec
$M_{\dot{r}}^P$	Dimensional y -moment derivative due to $\dot{\psi}_p$	#-ft/ft per sec
$N_{\dot{w}}^P$	Dimensional z -moment derivative due to \dot{w}_p	#-ft/ft per sec
$N_{\dot{r}}^P$	Dimensional z -moment derivative due to $\dot{\psi}_p$	#-ft/rad per sec
$F_x - F_y - F_z$	x - y - z components of lift and drag, prop. axes	#
F_T	Tangential force at average radius R	#
$M_x - M_y - M_z$	x - y - z components of moment, prop. axes	#-ft
$F_{x0} - M_{x0} - P_0$	Trim thrust, moment and horsepower	
$L-D$	Lift and drag forces	#
$X_{\Delta\delta}$	Dimensional x -force propeller coefficient due to $\Delta\delta$	#/rad
$X_{(\Delta\delta)^2}$	Dimensional x -force propeller coefficient due to $(\Delta\delta)^2$	#/rad ²
$X_{\delta_1^2}$	Dimensional x -force propeller coefficient due to δ_1^2 or δ_2^2	#/rad ²
Y_{δ}	Dimensional y -force propeller coefficient due to δ_2	#/rad
$Y_{\Delta\delta\delta}$	Dimensional y -force propeller coefficient due to $\Delta\delta \cdot \delta_2$	#/rad ²
Z_{δ}	Dimensional z -force propeller coefficient due to δ_1	#/rad
$Z_{\Delta\delta\delta}$	Dimensional z -force propeller coefficient due to $\Delta\delta \cdot \delta_1$	#/rad ²

		<u>Unit</u>
$K_{\Delta\delta}$	Dimensional κ -moment propeller coefficient due to $\Delta\delta$	#/rad
K_{δ_1}	Dimensional κ -moment propeller coefficient due to δ_1 or δ_2	#/rad ²
$K_{(\Delta\delta)^2}$	Dimensional κ -moment propeller coefficient due to $(\Delta\delta)^2$	#/rad ²
M_{δ}	Dimensional γ -moment propeller coefficient due to δ_1	#/rad
M_{δ_2}	Dimensional γ -moment propeller coefficient due to δ_2	#/rad
$M_{\Delta\delta \cdot \delta_2}$	Dimensional γ -moment propeller coefficient due to $\Delta\delta \cdot \delta_2$	#/rad ²
N_{δ}	Dimensional ζ -moment propeller coefficient due to δ_2	#/rad
N_{δ_1}	Dimensional ζ -moment propeller coefficient due to δ_1	#/rad
$N_{\Delta\delta \cdot \delta_1}$	Dimensional ζ -moment propeller coefficient due to $\Delta\delta \cdot \delta_1$	#/rad ²
λ_T	Propeller thrust parameter	nondimensional
λ_Q	Propeller torque parameter	nondimensional
λ_P	Propeller power parameter	nondimensional
P	Power	ft-#/sec
P_{HP}	Power	hp
\mathcal{P}	Nondimensional power	
\mathcal{T}	Propeller thrust coefficient	nondimensional
\mathcal{M}	propeller torque coefficient	nondimensional
\mathcal{F}	$\tan \delta$	nondimensional

Zero subscript denotes trim conditions, straight and level flight

f and a subscripts denote forward and aft conditions

G subscript denotes propeller control terms

IV

POSTULATED TANDEM PROPELLER SUBMARINE CONFIGURATION

4.1 HULL

The submarine configuration postulated for study in the Tandem Propeller Submarine program is shown in profile in Figure 4-1. The outline was taken from Reference (1) and is purported to be that of the Thresher submarine, SS(N)593. However, except for the general outline, all submarine configuration parameters are hypothetical.

In order to simplify the stability and control analyses two important assumptions were made relating to the submarine hydrostatics and its mass/inertia properties. These are:

- (1) The submarine is neutrally buoyant and trimmed at zero angles of attack and sideslip, in straight and level flight. The center-of-buoyancy is on the z -axis z_0 feet above the center-of-gravity (the origin of coordinates).
- (2) Mass and inertia properties are calculated on the basis of a homogeneous prolate spheroid. The sail is ignored in mass/inertia computations but included, where possible, in the determination of hydrodynamic properties.

The metacentric height \bar{z}_b was computed on the basis of a linear interpolation between submarines of lower and higher displacement (the Albacore and the George Washington). The distance from the forepoint to the c. g. was determined in the same way. The propeller planes were located as far from the c. g. as practical, at hull stations fore and aft, where the diameter is approximately 20 feet. For simplicity the distances l_{2f} and l_{2a} in Figure 1 were made equal.

The physical properties of the postulated TPS hull are summarized below:

		<u>Symbol</u>
Submerged displacement	: 4300 long tons (= weight)	$\Delta = W$
Length	: 275 feet	l
Max. diameter	: 32 feet	d
Fineness ratio	: 8.6	f
Distance, forepoint to c. g.	: 125 feet	l_1
Distance, prop. plane to c. g.:	110 feet, fore and aft	l_2
Metacentric height	: 1.0 feet	\bar{z}_b

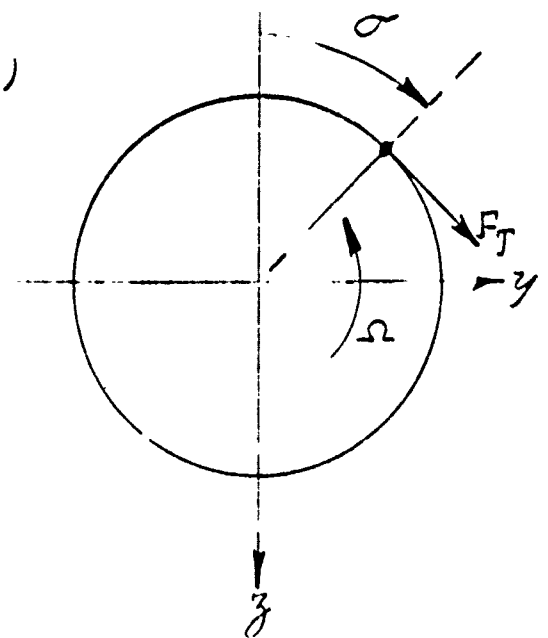
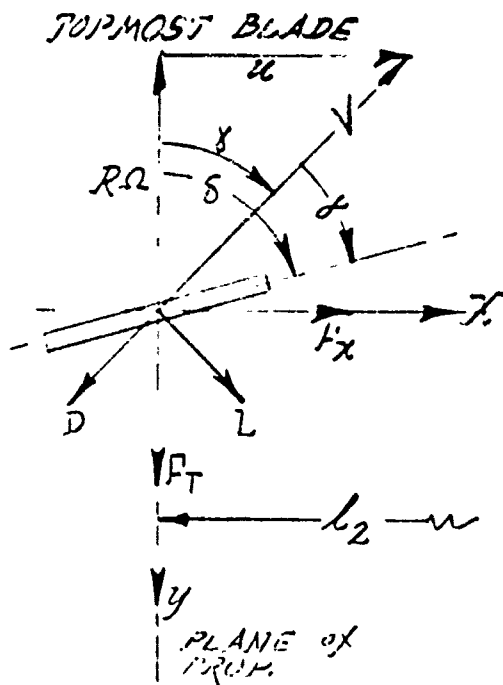
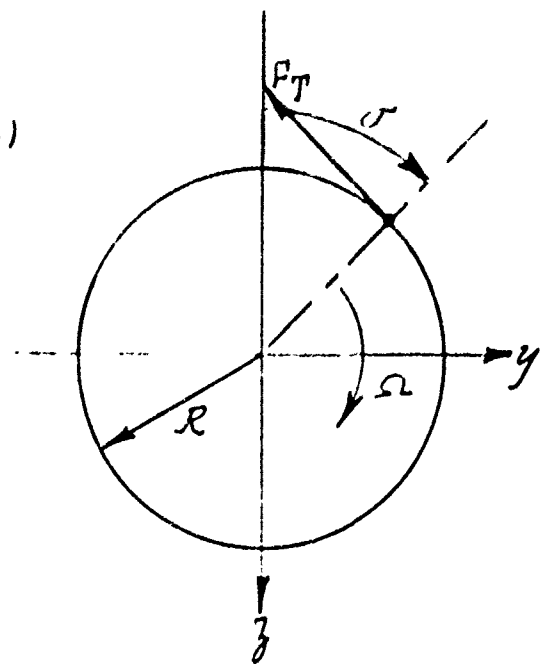
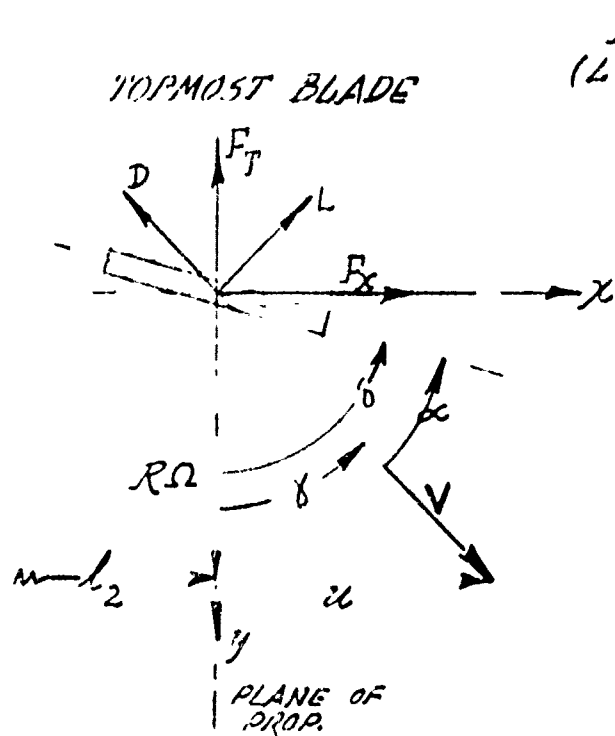
4.2 PROPELLERS

A hub diameter of 20 feet was assumed for both the forward and aft propellers and each propeller was assumed to be equipped with 16 blades with span 2 feet and chord 1.5 feet.

Propeller rotation is clockwise looking forward for the forward propeller and counterclockwise looking forward for the aft propeller. Propeller geometry is defined in Fig. 4-2 and the important propeller physical parameters are listed below.

		<u>Symbol</u>
Hub diameter	: 20 feet	
Tip diameter	: 24 feet	
Number of Blades:	16	<i>N</i>
Max. rpm	: 50	
Blade area	: 3 ft ²	<i>A</i>
Average radius	: 11 feet	<i>R</i>
Average diameter:	22 feet	<i>D</i>

Collective and cyclic components of blade pitch are shown in Figure 4-2.



$$\delta = \delta_0 + \Delta\delta + \delta_1 \sin\sigma + \delta_2 \cos\sigma$$

δ_0 TRIM COLLECTIVE PITCH
 $\Delta\delta$ CHANGE IN COLLECTIVE PITCH
 $\delta_1 = \delta_0 + \Delta\delta - \delta_0$

$$\left. \begin{array}{l} \delta_1 \sin\sigma \\ \delta_2 \cos\sigma \end{array} \right\} \text{CYCLIC COMPONENTS OF PITCH}$$

$\sigma = \beta \gamma$

FIGURE 4-2 - Propeller Sign Conventions

HYDRODYNAMIC ANALYSIS

5.1 GENERAL REMARKS

5.1.1 Task Objectives

The hydrodynamic analysis (summarized in this section) has the three-fold objective of determining the (1) stability coefficients, (2) control coefficients and (3) added-mass coefficients of the tandem-propeller submarine. Each of the three sets of coefficients derive from the force interaction between the proposed vehicle and its surrounding fluid medium. Traditionally, however, the stability coefficients are defined as those terms that yield the six-degree-of-freedom forces and moments acting on the vehicle as a result of the total velocity of the vehicle relative to the fluid. The control coefficients, on the other hand, define the six-degree-of-freedom forces and moments produced by whatever control mechanism is employed. In the case of the proposed vehicle, the basic control variables or inputs are the collective and cyclic pitch of the forward and aft propellers, respectively. The added-mass coefficients yield the forces and moments (for all six degrees of freedom) that are caused when the vehicle is accelerating with respect to its surrounding fluid medium. Since these forces are proportional to vehicle acceleration, both linear and angular, they sum with the inertia reaction terms in the equations of motion; hence, the origin of the term "added mass".

5.1.2 Problem Areas

The most straightforward procedure for obtaining the hydrodynamic characteristics of the tandem-propeller submersible, (the assumed geometry being given in Figure 4-1) would be model tests. Lacking test data such as would be obtained from a water tunnel, towing tank, or whirling arm facility, it is necessary to resort to theoretical predictions based on fluid mechanics analyses and to extrapolation of empirical data obtained for similar geometric forms.

Since the tandem-propeller submarine concept envisages the elimination of the usual fixed and movable planes and fins at the aft end of the vehicle, the hydrodynamic analysis resolves to a task of predicting the force and moment properties of a streamlined body of revolution as modified by the presence of a vertical fairwater and two counter-rotating propellers wrapped circumferentially around the forward and aft ends of the hull (see Figure 4-1). A sizeable number of practical and theoretical problems immediately arise. First of all, the stability coefficients of a body of revolution are determined in practice by those properties of a real fluid that make the application of potential-flow theory invalid. The flow about a slender body of revolution is characterized by a large boundary layer and flow separation, plus a wake. Thus, it is not possible to theoretically predict stability coefficients any more reliably than one can predict the drag coefficient. Lacking test data for the specific geometry assumed here, it is, however, possible to obtain stability coefficients by extrapolating from the body of test results obtained by previous investigators.

In addition to the problem of interaction between the flow produced by the fairwater and the three dimensional hull, there is the more serious problem of hull-propeller interaction. From Figure 4-1, it is seen that the flow over the hull will be influenced by the propellers and, concurrently, the flow field at the propellers will be influenced by the presence of the hull. The form and magnitude of these interactions depend, to a very large extent, on the magnitude of the forward velocity (u) of the submarine.

For the case of high forward speed, the assumption is made that the velocities induced by the propeller (both forward and aft of each propeller plane) are small relative to the forward velocity, U . Note that the axial component of these propeller-induced velocities will increase the axial flow velocity over the hull above that due to the free stream velocity. It was estimated that the propeller-induced axial velocity could become as large as twenty (20) percent of the free-stream velocity. Since the existing Reynold's number (approximately 10^7) indicates fully developed turbulent flow (such that the rate of change of force coefficient with velocity is small) it is believed that the error introduced by neglecting the influence of propeller-induced axial and tangential velocities on hull hydrodynamic forces is small. A similar conclusion can not be made for the case of low forward speed and the hover condition.

In addition to the influence of the propeller on the flow about the hull, there is the influence of the hull on the flow seen by the propeller. For motion of the submarine along the X axis only, the flow field is symmetrical at the plane of the propeller, with the flow velocities in the inviscid flow field near the hull being higher than the free stream velocity, U . This increase in the inviscid flow velocity is also accompanied by the presence of a boundary layer that reduces the fluid velocities seen by the propeller blades near the boundary of the hull. In the main, the departure from free-stream conditions is small for axial flow permitting the justifiable assumption that axial motion of the hull has no significant influence on the flow field existing at the plane of the propellers. A similar assumption can not be made for the case of transverse motion of the hull and the influence of the flow field (produced by transverse velocities) on the stability coefficients of the propellers is discussed below in Section 5.2.1.2.2.

The phenomenon of propeller interaction is also deserving of attention. In the case of high forward speed, the previous assumption that the propeller-induced velocities are small relative to the free-stream velocity also says that the wake of the forward propeller has little influence on the flow field existing at the plane of the aft propeller. As the tandem propeller submarine proceeds from high- to low-forward speed operation, this assumption of zero interaction between pro-

propellers becomes untenable. A qualitative discussion of the influence of the wake of the forward propeller upon the aft propeller is given in Reference (2). Some of the propeller interaction phenomena existing at zero (hover) speed are discussed below in Section 5.2.2.2.

5.2 STABILITY COEFFICIENTS OF THE TPS

The stability coefficients that define the forces and moments acting on the TPS as a result of its total linear and angular velocity are derived separately for the cases of high and low (or zero) forward speeds. It will be seen that for the low speed or hover case, the stability characteristics of the propellers can not be derived in coefficient form nor can the stability forces and moments be separated from the forces and moments produced by the control variables, collective and cyclic pitch.

5.2.1 High-Speed Case

5.2.1.1 Hull Plus Fairwater Contribution

5.2.1.1.1 Evaluation Technique

The drag coefficient of the TPS hull was derived from the experimental data presented in Reference (3). This reference presents data for a series of bodies of revolution that are similar to submarine hulls. In view of the uncertainty in exact geometry of the TPS hull form, the drag coefficient was assumed to be the average of the drag coefficients presented in Reference (3) for zero angle of attack. The influence of speed on drag was not determined in these tests which were conducted at a constant Reynolds number of 3.1×10^6 . Since this Reynolds number is sufficiently large to insure fully developed turbulent flow (similar to that over the full-scale hull), the variation of drag coefficient with

It is recognized that the TPS performance computed for a specified installed horsepower will be a sensitive function of this assumed drag coefficient.

velocity can be justifiably neglected in the high-speed case.

As mentioned above in Section 5.12, it is not practical to theoretically evaluate the stability coefficients of a slender body of revolution. Hence, experimental data were utilized to the extent that such data were available. Reference (4) presents some "build-up" data for an early Fleet Ballistic Missile (FBM) Submarine configuration with a fineness ratio (length of hull/maximum diameter) of 11.3. The hull form and fineness ratio were deemed sufficiently close to the postulated TPS geometry (fineness ratio of 8.6) to justify the use of these data. The stability coefficients of the hull were obtained by operating on the data using graphical methods. In addition, the force and moment contributions of the assumed fairwater (see Figure 4-1) were determined using the low-aspect-ratio hydrofoil theory presented in Reference (5). The fairwater (sail) was assumed to be a flat plate and the aspect ratio was determined by correcting the span for the effects of hull proximity. The computational details are not included in this report.

5.2.1.1.2 Tabulation of Results

The results of the above analysis were placed in non-dimensional coefficient form in order to facilitate comparison of the hydrodynamic characteristics of the TPS with those of conventional submarines possessing stabilizing planes at the aft end. Table 5-1 summarizes the non-dimensional stability coefficients of the TPS minus the fore and aft propellers and compares them with the coefficients of the Albacore. The most notable difference between the Albacore and the TPS is the Albacore's significantly larger damping in pitch and yaw (M'_δ and N'_r) and vertical force (Z) due to vertical velocity (w) and pitching velocity ($\dot{\theta}$).

TABLE 5-1		
Non-Dimensional Hull Derivatives (TPS & Albacore)		
Derivative	TPS	Albacore
K'_p	$-(46.6 + 6.36/p') \times 10^{-6}$	-59.6×10^{-6}
K'_{α}	$-(122.8 + 76.8/r') \times 10^{-6}$	-216×10^{-6}
K'_{ν}	$-(561 + 1610/\nu') \times 10^{-6}$	$-.00215$
M'_{ω}	$+0.00692$	$.00652$
M'_g	$-.00039$	$-.00412$
N'_p	$-(12.1 + 16.75/p') \times 10^{-6}$	-84.9×10^{-6}
N'_{α}	$-(716 + 102/r') \times 10^{-6}$	$-.00274$
N'_{ν}	$-.0086$	$-.01183$
X'_{ω}	$-.00102$	
Y'_{ν}	$-.0209$	$-.0395$
Y'_{α}	$-[495 + 937/r'] \times 10^{-6}$	$.00599$
Y'_p	$-[554 + 76.8/p'] \times 10^{-6}$	$-.000614$
Z'_{ω}	$-.00497$	$-.0215$
Z'_g	$-.00066$	$-.00978$

Note: $r' = R^2/U$; $p' = P^2/U$; $\nu' = \nu/U$

TABLE 5-1 - Tabulation of Nondimensional Hull Derivatives (TPS and Albacore)

5.2.1.2 Propeller Contribution

Any departure of the submarine from a steady course (represented by a fixed value of axial velocity, u) results in changes of flow through the tandem propellers and consequent force and moment inputs from the propeller to the hull. Specifically, when the propeller has motion other than along its x axis, it is seen that the advance ratio will vary around the circumference of the propeller. These variations in advance ratio will produce force distributions on the propeller disc similar to the distributions produced by cyclic pitch. Forces and moments will result that oppose the disturbance motions and various cross-coupling forces and moments will appear, e.g., pitching moment due to sideslip. Although an analysis has been performed to derive the stability coefficients of a propeller in such a manner that the analysis is valid for the complete speed regime (see Section 5.2.2), the work of Glauert has been employed to obtain the high speed stability coefficients of the large-diameter-to-hub-ratio propellers employed on the TPS.

5.2.1.2.1 Results Obtained by Glauert

In Reference (6), Glauert derived the stability coefficients of an isolated propeller (no hub or center body) for the case where the disturbance velocities ($\bar{u}, \bar{v}, \bar{w}, \dot{\varphi}, \dot{\theta}, \dot{\psi}$) are small relative to the free-stream equilibrium velocity, u_0 . This analysis assumed the propeller blade angle, δ , to be fixed and the load distribution on the blade to be known. Two forms of engine-power function were considered. One function states that the ratio of engine power to engine rpm is fixed (i.e., $P/2\pi n = \text{a constant}$); the second function states that engine power is varied to maintain propeller rpm fixed. In the latter case, the speed-torque characteristics of the engine do not enter into the derivation of the stability coefficients.

Table 5-2 summarizes the stability derivatives of a propeller as obtained by Glauert who used blade-element theory and neglected the influence of inflow and swirl. The lambda parameters shown in this table are defined by Glauert as -

$$\lambda_T = \frac{1}{2} \frac{\dot{\tau}}{\tau} \frac{d\tau}{d\dot{\tau}}$$

$$\lambda_Q = \frac{1}{2} \frac{\dot{\mu}}{\mu} \frac{d\mu}{d\dot{\mu}}$$

$$\lambda_P = \frac{1}{2} \left(1 - \beta\right) \frac{dP}{d\beta}$$

where $\dot{\tau} = \frac{u_0}{\Omega R} = \tan \gamma$

and τ and μ are the thrust and torque coefficients, respectively, of the propeller. On using blade-element theory, these thrust and torque coefficients can be expressed as

$$\tau = \frac{F_{th}}{\frac{1}{2} \rho A N \Omega^2 R^2} = \sqrt{1 + \dot{\tau}^2} \left\{ C_{L\alpha} (\delta - \gamma) - \dot{\tau} [C_{D_0} + f_1 C_{L\alpha}^2 (\delta - \gamma)^2] \right\}$$

$$\mu = \frac{M_{to}}{\frac{1}{2} \rho A N \Omega^2 R^3} = \sqrt{1 + \dot{\tau}^2} \left\{ C_{L\alpha} (\delta - \gamma) \dot{\tau} + [C_{D_0} + f_1 C_{L\alpha}^2 (\delta - \gamma)^2] \right\}$$

Since propeller rpm will be considered as fixed in the subsequent stability and control analyses, it is only necessary to evaluate the λ_T and λ_Q parameters by properly formulating the derivatives of the thrust- and torque-coefficient expressions. Accordingly, the λ_T and λ_Q parameters have been evaluated as -

$$\lambda_T = \frac{1}{2} \frac{\dot{\tau}}{1 + \dot{\tau}^2} \frac{C_{L\alpha} [\dot{\tau}(\delta - \gamma) - 1] - C_{D_0} [1 - 2\dot{\tau}^2] + f_1 C_{L\alpha}^2 (\delta - \gamma) [2\dot{\tau} - (\delta - \gamma)]}{C_{L\alpha} (\delta - \gamma) - \dot{\tau} C_{D_0} - \dot{\tau} f_1 C_{L\alpha}^2 (\delta - \gamma)^2}$$

$$\lambda_Q = \frac{1}{2} \left\{ \frac{\dot{\tau}^2}{1 + \dot{\tau}^2} + \frac{\dot{\tau}}{1 + \dot{\tau}^2} \frac{C_{L\alpha} (\delta - \gamma) (1 + \dot{\tau}^2) - \dot{\tau} C_{D_0} - 2f_1 C_{L\alpha}^2 (\delta - \gamma)}{\dot{\tau} C_{L\alpha} (\delta - \gamma) + C_{D_0} + f_1 C_{L\alpha}^2 (\delta - \gamma)^2} \right\}$$

Note also that the parameter, k_2 , appearing in Table 5-1, is obtained from the following relationship appearing in Reference 6:

$$N \int_{\text{blade-root radius}}^{\text{blade-tip radius}} a r^2 dr = k_2 4 R^2 F_T$$

$$\text{where } F_T = N \int_{\text{blade-root radius}}^{\text{blade-tip radius}} a dr$$

a = thrust per unit length of blade

r = radial distance along blade

In order to apply Glauert's results to the calculation of propeller stability coefficients, one must establish, first, the trim conditions of speed (U_0), thrust and torque (F_{T_0} and M_{T_0}), blade pitch angle (δ_0), and blade flight-path angle (γ_0). Also required are the slope of the lift curve and drag coefficient of the individual blade elements. These basic hydrodynamic quantities were evaluated by assuming each propeller blade to be isolated and, effectively, a semi-wing. The curvature of the wall (hull) was neglected and the lift-curve slope was evaluated for the blade geometry described earlier by making the classical aspect ratio correction (see Reference (7)). The following blade hydrodynamic characteristics were obtained:

$$C_{L_1} = 3.59$$

$$C_{D_0} = .015$$

$$f_i = .119$$

5.2.1.2.2 Effect of Transverse Flow Around Hull

As mentioned in Section 5.1.2, the flow field at the propeller plane when the propeller has a transverse velocity relative to the fluid will be altered by the presence of a body of revolution centered within the propeller disc. The local flow, as caused by the presence of the center body, can be approximated reasonably

well by evaluating the two-dimensional potential flow around the circular cross section of the hull. The local flow velocity caused by either a heaving or side-slipping velocity, w or v , is given by (see Reference (8)) -

$$w_{\text{local}} = 2 w_p \sin \sigma$$

$$v_{\text{local}} = 2 v_p \cos \sigma$$

where w_p and v_p refer to the velocity of the propeller as defined at the origin of an axis system fixed in the plane of the propeller. Note that the local velocity varies around the hull as a sine or cosine function of the blade azimuth angle, σ , in the same manner that the free-stream velocities, w_p and v_p , alter the tangential velocity in a blade element when no center body is present. In view of the identical functional form, the integration process involved in summing the forces on one blade over a complete traversal of azimuth angle, σ , is not altered but there is a twofold increase in stability forces caused by transverse velocity when a center body is present. This correction has been applied to the derivatives $Y_{\dot{v}}^P$, $M_{\dot{v}}^P$, $Z_{\dot{w}}^P$, and $N_{\dot{w}}^P$ shown in Table 5-2.

5.2.1.2.3 Tabulation of Results

The above presented stability coefficients apply to one propeller only and to propeller axes, where these axes are parallel to body axes but have their origin at $x = l_2$, fore and aft. Thus, the following relationships must be used to sum the contributions from the fore and aft propellers such that the combined coefficients or derivatives refer to motions of the c. g. of the TPS:

$$\bar{u}_p \Big]_{f,2} = \bar{u} ; \quad \bar{v}_p \Big]_f = \bar{v} + \dot{\psi} l_2 ; \quad \bar{v}_p \Big]_a = \bar{v} - \dot{\psi} l_2$$

$$\bar{w}_p \Big]_f = \bar{w} - \dot{\theta} l_2 ; \quad \bar{w}_p \Big]_a = \bar{w} + \dot{\theta} l_2$$

$$\dot{\psi} \Big]_{f,2} = \dot{\psi} ; \quad \dot{\theta} \Big]_{f,2} = \dot{\theta} ; \quad \dot{\psi} \Big]_{f,2} = \dot{\psi}$$

TABLE 5-2	
Tabulation of Propeller Derivatives (One Propeller)	
Clockwise Rotation Looking Forward	Sign Change for Counterclockwise Rotation
$X_u^p = +2F_{x0}f_1(\bar{\lambda})/u_0$	No
$X_p^p = +2F_{x0}f_2(\bar{\lambda})/\Omega$	Yes
$Y_v^p = -2 M_{x0} (1-\bar{\lambda}_q)/\Omega R^2$	No
$Y_\delta^p = + M_{x0} \bar{\lambda}_q/u_0$	Yes
$Z_w^p = Y_v^p$	/
$Z_r^p = Y_\delta^p$	/
$K_p^p = -2 M_{x0} f_3(\bar{\lambda})/\Omega$	No
$K_u^p = +2 M_{x0} f_4(\bar{\lambda})/u_0$	Yes
$M_v^p = -2F_{x0}(1-\bar{\lambda}_T)/\Omega$	Yes
$M_\delta^p = k_2 F_{x0} D^2 \bar{\lambda}_T M_0$	No
$N_w^p = M_v^p$	/
$N_r^p = M_\delta^p$	/

$f(\bar{\lambda})$	CONSTANT P/Ω	CONSTANT Ω
$f_1(\bar{\lambda})$	$\bar{\lambda}_p(1+\bar{\lambda}_p) - \bar{\lambda}_q / 1 + \bar{\lambda}_p - \bar{\lambda}_q$	$\bar{\lambda}_T$
$f_2(\bar{\lambda})$	$\bar{\lambda}_p(1-\bar{\lambda}_T) / 1 + \bar{\lambda}_p - \bar{\lambda}_q$	$1 - \bar{\lambda}_T$
$f_3(\bar{\lambda})$	$\bar{\lambda}_p(1-\bar{\lambda}_q) / 1 + \bar{\lambda}_p - \bar{\lambda}_q$	$1 - \bar{\lambda}_q$
$f_4(\bar{\lambda})$	$\bar{\lambda}_p \bar{\lambda}_q / 1 + \bar{\lambda}_p - \bar{\lambda}_q$	$\bar{\lambda}_q$

TABLE 5-2 - Tabulation of Propeller Derivatives (One Propeller)

The total stability forces and moments produced by the propellers are thus:

$$\sum X_p = X_u^p \Big]_{f,r} \bar{u} + X_\phi^p \Big]_{f,r} \dot{\psi}$$

$$\sum Y_p = Y_{\bar{v}}^p \Big]_f (\bar{v} + \dot{\psi} l_2) + Y_{\bar{v}}^p \Big]_a (\bar{v} - \dot{\psi} l_2) + Y_\theta^p \Big]_{f,r} \dot{\theta}$$

$$\sum Z_p = Z_{\bar{w}}^p \Big]_f (\bar{w} - \dot{\theta} l_2) + Z_{\bar{w}}^p \Big]_a (\bar{w} + \dot{\theta} l_2) + Z_{\dot{\psi}}^p \Big]_{f,r} \dot{\psi}$$

$$\sum K_p = K_\phi^p \Big]_{f,r} \dot{\psi} + K_u^p \Big]_{f,r} \bar{u}$$

$$\begin{aligned} \sum M_p = & M_{\bar{v}}^p \Big]_f (\bar{v} + \dot{\psi} l_2) + M_{\bar{v}}^p \Big]_a (\bar{v} - \dot{\psi} l_2) - Z_{\bar{w}}^p \Big]_f (\bar{w} - \dot{\theta} l_2) l_2 \\ & + Z_{\bar{w}}^p \Big]_a (\bar{w} + \dot{\theta} l_2) l_2 - Z_Y^p \Big]_f \dot{\psi} l_2 + Z_Y^p \Big]_a \dot{\psi} l_2 + M_\theta^p \Big]_{f,r} \dot{\theta} \end{aligned}$$

$$\begin{aligned} \sum N_p = & Y_{\bar{v}}^p \Big]_f (\bar{v} + \dot{\psi} l_2) l_2 - Y_{\bar{v}}^p \Big]_a (\bar{v} - \dot{\psi} l_2) l_2 + N_{\bar{w}}^p \Big]_f (\bar{w} - \dot{\theta} l_2) \\ & + N_{\bar{w}}^p \Big]_a (\bar{w} + \dot{\theta} l_2) + Y_\theta^p \Big]_f \dot{\theta} l_2 - Y_\theta^p \Big]_a \dot{\theta} l_2 + N_r^p \Big]_{f,r} \dot{\psi} \end{aligned}$$

If it is assumed that the fore and aft propellers are symmetrical and are operated at a constant propeller speed with the forward propeller turning clockwise and the aft propeller turning counterclockwise, then insertion of the proper propeller coefficients (from Table 5-2) into the above force and moment summations produces the following results:

$$\sum X_p = \left[\frac{4 F_{x_0}}{u_0} \lambda_T \right] \bar{u}$$

$$\sum Y_p = \left[- \frac{4 |M_{x_0}| (1 - \lambda_Q)}{\Omega R^2} \right] \bar{v}$$

$$\sum Z_p = \left[- \frac{4 |M_{x_0}| (1 - \lambda_Q)}{\Omega R^2} \right] \bar{w}$$

$$\sum K_p = \left[- \frac{4 |M_{x_0}| (1 - \lambda_Q)}{\Omega} \right] \dot{\psi}$$

$$\sum M_p = \left[- \frac{4 F_{x_0} (1 - \lambda_T) l_2}{\Omega} - \frac{2 |M_{x_0}| \lambda_Q l_2}{u_0} \right] \dot{\psi}$$

$$+ \left[2 k_2 F_{x_0} \frac{D^2}{u_0} \lambda_T - \frac{4 |M_{x_0}| (1 - \lambda_Q) l_2^2}{\Omega R^2} \right] \dot{\theta}$$

$$\sum N_p = \left[\frac{4 F_{x_0} (1 - \lambda_T) l_2}{\Omega} + \frac{2 |M_{x_0}| \lambda_Q l_2}{u_0} \right] \dot{\theta}$$

$$+ \left[2 k_2 F_{x_0} \frac{D^2}{u_0} \lambda_T - \frac{4 |M_{x_0}| (1 - \lambda_Q) l_2^2}{\Omega R^2} \right] \dot{\psi}$$

The above force and moment summations are expressed in terms of the trim thrust and torque (F_{T_0} and M_{T_0}) of a single propeller and in terms of other trim quantities such as α_0 , Ω , λ_T , λ_Q , and k_2 . For unbalanced operation of the propellers, the above summations are not valid but must be rederived taking into account differences (between the forward and aft propellers) in

F_{T_0} , M_{T_0} , Ω , and the lambda parameters which, in turn, are functions of γ and δ .

5.2.1.3 Combined (Hull-Propeller) Coefficients

The stability characteristics of the hull-propeller combination can be put into derivative form such that the equations of motion reduce to their simplest form. Since the hull stability derivatives have been tabulated in non-dimensional form and the propeller forces and moments have been evaluated in dimensional form, the decision was made to dimensionalize the hull derivatives and to sum these derivatives with their propeller counterparts. Accordingly, a set of dimensional stability coefficients is obtained based on perturbation velocities such that the total hydrodynamic force and moment acting on a TPS (exclusive of control forces) can be expressed as follows:

$$\left. \begin{aligned}
 \sum X &= +X_u \bar{u} \\
 \sum Y &= Y_v \bar{v} + Y_r \dot{\psi} + Y_p \dot{\phi} \\
 \sum Z &= Z_w \bar{w} + Z_q \dot{\theta} \\
 \sum K &= K_v \bar{v} + K_p \dot{\phi} + K_r \dot{\psi} + M_\theta \cos \theta \sin \phi \\
 \sum M &= M_w \bar{w} + M_q \dot{\theta} + M_r \dot{\psi} + M_\theta \sin \phi \\
 \sum N &= N_v \bar{v} + N_p \dot{\phi} + N_q \dot{\theta} + N_r \dot{\psi}
 \end{aligned} \right\} (5-0)$$

The derivatives in the above equations are defined and tabulated in Table 6-2.

5.2.2 Hovering Case

5.2.2.1 General Remarks

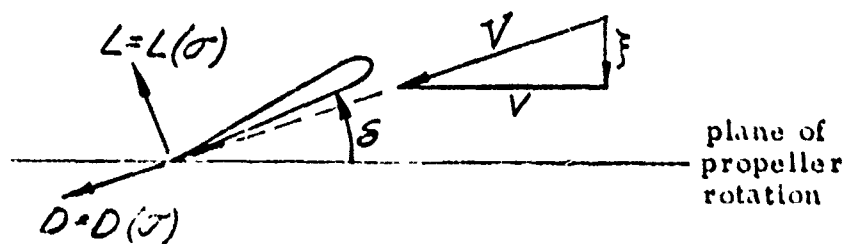
The propeller forces and moments plus hull forces and moments produced as a function of velocity disturbance variables for the case where U_0 is small or zero are derived in this section. It should be noted that the below hydrodynamic analysis is preliminary and should be considered tentative until such time that these results can be checked further. One drawback with the analysis, at the present time, is that the definitions and terminology used in Reference (9) are employed rather than that employed in the remainder of this report. Nevertheless, the results serve to indicate the general nature of the problems that will be encountered in performing a stability and control analysis for the hover condition.

The analysis made to evaluate the low-speed propeller forces is based on an analytical procedure believed to be sufficiently general that it permits the derivation of propeller forces and moments throughout the speed regime. Only the low-speed solution is given here, however. To avoid mathematical detail, only the bare outline of the procedure is given with the final result obtained for the X -force presented in the body of the report. The remaining five force and moment expressions are given in an appendix.

A tentative formulation is made of the forces and moments produced by the hull at low speeds. When this analysis is refined and reduced to a quantitative basis, it is anticipated that these body (hull) forces will be small relative to the forces produced by the tandem propellers.

5.2.2.2 Propeller Forces

With reference to the following sketch, blade-element theory yields:



$$L(\sigma) = \frac{1}{2} \rho A V(\sigma)^2 C_{L\alpha} \left[\delta(\sigma) - \tan \bar{\eta}' \frac{\dot{f}(\sigma)}{V(\sigma)} \right] \quad (5-1)$$

$$D(\sigma) = \frac{1}{2} \rho A V(\sigma)^2 \left[C_{D0} + f C_{L\alpha}^2 \left\{ \delta(\sigma) - \tan \bar{\eta}' \frac{\dot{f}(\sigma)}{V(\sigma)} \right\}^2 \right] \quad (5-2)$$

where $V(\sigma)$ = total (local) water velocity relative to the blade, ft/sec.

$V(\sigma)$ = local tangential velocity relative to the blade in the plane of the propeller, ft/sec.

$\dot{f}(\sigma)$ = local axial velocity relative to the blade, ft/sec.

In contrast to the assumptions made for the high-speed case, namely, that (1) propeller forces caused by disturbance velocities are independent of the blade angles of attack caused by changes in blade pitch angle, δ , and (2) changes in blade angle of attack produced by pitch-angle change cause variations in propeller-induced flow that are negligible relative to the free-stream velocity, u_0 , it is necessary to include all sources whereby V , V , \dot{f} , and δ vary around the circumference of the propeller as a function of the blade azimuth angle, σ . Both cyclic pitch and body (hull) motions will cause perturbations in \dot{f} and V and, hence, in the total velocity, V . Consideration of the prevailing kinematics and geometry yields the following for the local axial and tangential velocity components:*

*The zero reference for the blade azimuth angle, σ , is the positive y axis as in Reference 9.

$$f(\sigma) = u + f_i + gR \sin \sigma - rR \cos \sigma \quad (5-3)$$

$$V(\sigma) = (\Omega - p)R + (v + r l_2) \sin \sigma - (w - g l_2) \cos \sigma$$

where

f_i = propeller-induced axial inflow velocity resulting from momentum change through the propeller

Note that $\gamma(\sigma) = \tan^{-1} \frac{f(\sigma)}{V(\sigma)}$ (5-4)

When $u = u_0$ (large value) and $v = w = p = g = r = 0$, f_i is assumed negligible, and Equations (5-3) and (5-4) reduce to

$$\gamma_0 = \tan^{-1} \frac{u_0}{\Omega R}$$

Equations (5-1) and (5-2) for lift and drag, together with Equation (5-3), yield the instantaneous force on a single blade as a function of blade azimuth angle, where the blade angle of attack and the total water velocity relative to the blade vary continuously around the circumference of the hull. Since the frequencies at which the hull responds as a rigid body are extremely low compared to the frequency of propeller rotation, it is evident that only the average force exerted by a propeller blade will affect the hull motions*. The average force per revolution of a single blade times the number of blades is the same as the summation of the forces on each blade at a given instant of time. For example, the total average axial force, F_x , can be obtained by the following integration:

$$F_x = \frac{N}{2\pi} \int_0^{2\pi} [L(\sigma) \cos\{\gamma(\sigma)\} - D(\sigma) \sin\{\gamma(\sigma)\}] d\sigma \quad (5-5)$$

where

N = number of blades

*Statement is true in the stability sense. Hull vibrations are, however, very much a function of the periodic propeller forces even though the mean value may reduce to zero.

The integration procedure indicated in Equation (5-5) would be used, in similar fashion, to derive the remaining force and moment components produced by the propeller.

Examination of the blade-force equations (lift and drag) indicates that they are nonlinear, for example, in ξ and V . The above indicated integration is facilitated by linearizing the terms in the force equations about the trim speed. Expansion of γ (i.e., the inverse tangent expression, $\tan^{-1} \frac{\xi}{V}$) in a Taylor's series and linearizing by retaining only the constant and linear terms leads to:

$$\tan^{-1} \frac{\xi}{V} \approx \tan^{-1} \left(\frac{u_0}{\Omega R} \right) + \frac{1}{1 + \left(\frac{u_0}{\Omega R} \right)^2} \left[\frac{\xi}{V} - \frac{u_0}{\Omega R} \right]$$

where u_0 is the trim equilibrium speed. At the trim advance ratio, $\frac{u_0}{\Omega R}$, of 1.0 this expansion gives good accuracy in the range $0.85 < \frac{u_0}{\Omega R} < 1.15$. Similarly, the total velocity, V , can be approximated by means of the binomial expansion:

$$V = \sqrt{V^2 + \xi^2} = V \sqrt{1 + \left(\frac{\xi}{V} \right)^2}$$

$$V \approx V \sqrt{1 + \left(\frac{u_0}{\Omega R} \right)^2} \left\{ 1 + \frac{\left(\frac{\xi}{V} \right)^2 - \left(\frac{u_0}{\Omega R} \right)^2}{2 \left[1 + \left(\frac{u_0}{\Omega R} \right)^2 \right]} \right\}$$

In the case of the inverse tangent expansion, the quantity $\left[\frac{\xi}{V} - \frac{u_0}{\Omega R} \right]$ is treated as a small quantity and in the case of the total velocity expansion, the quantity $\left[\left(\frac{\xi}{V} \right)^2 - \left(\frac{u_0}{\Omega R} \right)^2 \right]$ is treated as a small quantity. In these expansions, only first powers in the motion variables, ϕ , θ , γ , $u - u_0$, v , and w , are retained. Products of these terms are also neglected in the derivation of the final force and moment expressions.

Evaluation of the induced inflow velocity, ξ_i , can be carried out by means of a combined lifting line and propeller momentum analysis. As a consequence, ξ_i can be expressed as a function of the trim collective pitch, δ_0 , where the total pitch angle of the blade is defined (similar to Reference (9)) as:

$$\delta(\sigma) = \delta_0 + a_1 \sin \sigma + b_1 \cos \sigma$$

The above procedure is equivalent to stating that the induced velocity and thrust change with the collective pitch angle without lag. Effects of the cyclic pitch on the induced velocity are neglected and the cascade effects are neglected. Note that the adequacy of the first assumption (neglecting the effects of cyclic pitch) depends on the operating condition. It is a good assumption for high speeds where the propellers are operating at high thrust levels and is a reasonable assumption for that low speed (or hover) case in which the propellers are operated at high thrust levels by "bucking" one propeller against the other. It is possible that further analytical work could permit one to relax these assumptions.

For the case of low or zero forward speed, the terms in the blade force equations are linearized about $u_0 = 0$. The expansions and integrations have been carried to completion for the low speed case and the results for the six forces and moments are presented in an appendix. The result obtained for the X force is given below. Note that this expression is not valid when $(u + \xi_i)$ approaches zero - a possible operating condition when the thrusts of the propellers are opposed at low speeds.

$$\begin{aligned}
 X_f = \frac{PNA}{2} R^2 \Omega^2 & \left\{ C_{L\alpha} \left[\delta_0 \left(1 + 2 \frac{r}{R} \right) - \frac{u + \xi_i}{R\Omega} + 2a_1 \frac{w - g l_2}{R\Omega} \right. \right. \\
 & \left. \left. - 2b_1 \frac{w + r l_2}{R\Omega} \right] \right. \\
 & - C_{D_0} \left(\frac{u + \xi_i}{R\Omega} \right) \\
 & \left. - f C_{L\alpha}^2 \left[\delta_0 \left(\delta_0 \frac{u + \xi_i}{R\Omega} - 2 \frac{r}{R} + b_1 \frac{r}{R} \right) \right. \right. \\
 & \left. \left. + \frac{u + \xi_i}{R\Omega} \left(\frac{a_1^2 + b_1^2}{2} \right) \right] \right\}
 \end{aligned}
 \tag{5-6}$$

where

$$\frac{\xi_i}{R\Omega} = \frac{b C_{L\alpha}}{8 - 2\delta_0 b C_{L\alpha}} \left[-1 + \sqrt{1 + \frac{16\delta_0 - 4\delta_0^2 b C_{L\alpha}}{b C_{L\alpha}}} \right]$$

$$b = \frac{NA}{\pi(R_{TIP}^2 - R_{ROOT}^2)} \approx \frac{NC}{2\pi R}$$

C = mean blade chord

yielding

$$\frac{\xi_i}{R\Omega} \approx 0.858\delta_0 - 0.600\delta_0^2$$

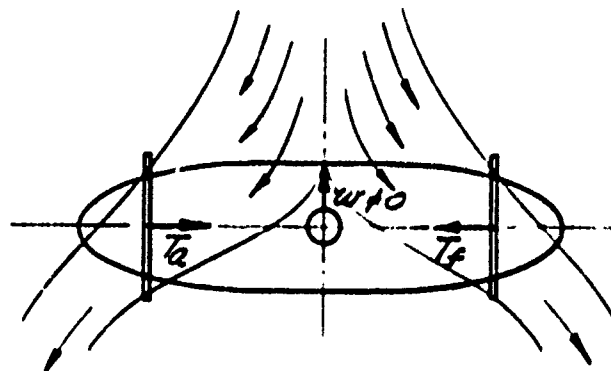
Examination of Equation (5-6) shows that there is coupling between control deflections and motions of the hull. As will also be shown later for the high speed case, there are cross couplings between the various components of control deflections. Accordingly, Equation (5-6), (plus the Appendix) indicates that a stability and control analysis of the hovering case will be extremely complicated, unless the indicated coupling effects can be shown to be small for reasonable values of control inputs. These questions will be resolved during the remainder of this study.

5.2.2.2.1 Possible Modes of Operation at Low Speed

Considerable flexibility exists in the choice of a low speed mode of operation. These include at least the following:

- (1) Front prop thrusting, rear prop non-rotating but trimmed to counteract torque
- (2) Rear prop thrusting, front prop non-rotating but trimmed to counteract torque
- (3) Both props thrusting
- (4) Front prop thrusting, rear prop counter-thrusting
- (5) Rear prop thrusting, front prop counter-thrusting

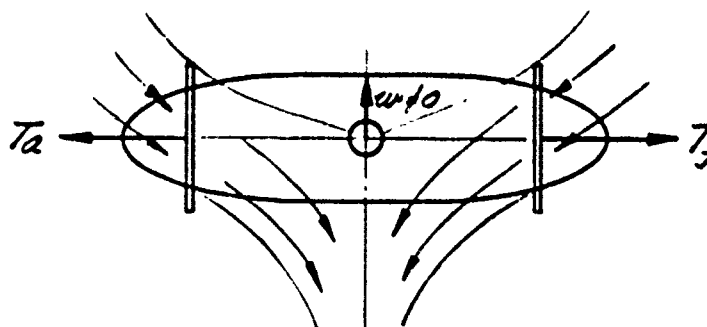
These cases may have quite different stability and control characteristics and probably are quite different with respect to vibrations that would be induced. This latter point can be visualized by considering two possible modes of vertical translation at zero axial speed as shown on the following sketch:



$$T_f = T_a$$

$$u = 0$$

Sketch 5a



$$T_f = T_a$$

$$u = 0$$

Sketch 4a

In Sketch (4a) the wakes of the propellers approach each other. This would cause a confused vortical distribution near the hull with possibilities for exciting hull vibrations and propeller vibrations.

In Sketch (5a) the flow over the major portion of the hull is non-vortical, and the wakes from the two propellers do not approach each other. Hence, the latter appears to be the more desirable from the vibration viewpoint.

5.2.2.3 Hull forces and Moments

The hull forces and moments for the low speed or hovering cases are different from those for the high speed case. In the low speed case the velocity $U = \sqrt{u^2 + v^2 + w^2}$ is very small. The lift (i.e., side force) generated by the fairwater will be extremely nonlinear and is omitted here. The predominant terms probably arise from the cross flow velocities, v and w . In this case, viscous cross flow theory can be used and the drag components resulting from the velocities considered independently. These forces will also be nonlinear and small but at least they can be defined with moderate accuracy. Their inclusion is necessary for the definition of trim conditions when $u = 0$. The following force expressions are obtained:

$$X_{u_{HULL}} = \frac{1}{2} C_{D1} \rho A_1 u^2$$

$$Y_{v_{HULL}} = \frac{1}{2} C_{D2} \rho A_2 v^2 + \frac{1}{2} C_{D3} \rho A_3 v^2$$

$$Z_{w_{HULL}} = \frac{1}{2} C_{D2} \rho A_2 w^2$$

where:

C_{D1} = viscous skin friction drag coefficient for the hull

A_1 = projected frontal area of hull plus sail

u = velocity component along x axis

ρ = density of fluid medium

C_{D2} = viscous cross flow drag coefficient for the hull

A_2 = projected side area of the hull (assumed to be a body of revolution)

C_{D3} = drag coefficient for the sail in transverse flow (assumed to be a flat plate)

A_3 = projected side area of the sail.

Let $A_1 = \frac{\pi d_m^2}{4} + bt$

$$A_2 = \int_{x=0}^{x=L} d(x) dx$$

$$A_3 = b-c$$

d_m = maximum hull diameter

b = height of sail above hull

t = thickness of sail airfoil

$d(x)$ = diameter of hull at station x

C = chord of the sail

Then

$$X_{u_{HULL}} = \frac{1}{2} C_{D1} \rho u^2 \left(\frac{\pi d_m^2}{4} + bt \right)$$

$$Y_{u_{HULL}} = \frac{1}{2} C_{D2} \rho u^2 \int_0^L d(x) dx + \frac{1}{2} C_{D3} \rho u^2 b-c$$

$$Z_{u_{HULL}} = \frac{1}{2} C_{D2} \rho u^2 \int_0^L d(x) dx$$

and the terms like X_w, Y_w, \dots are zero.

The moment expressions become

$$K = R_1 \frac{1}{2} C_{D3} \rho u^2 b-c$$

$$M = \frac{1}{2} C_{D2} \rho u^2 \int_0^L d(x) x dx$$

$$N = \frac{1}{2} C_{D2} \rho u^2 \int_0^L d(x) x dx + R_2 \frac{1}{2} C_{D3} \rho u^2 b-c$$

where R_1 = normal distance from x axis to center of pressure of the sail

R_2 = normal distance from y axis to center of pressure of the sail.

The drag coefficients must be properly evaluated, taking into account the configuration of the hull and the Reynold's number. It would be very desirable to have experimental data for the drag coefficients but in view of the lack of such values, classical drag data for flat plates and cylinders must be used*. Also the expression for $d(\gamma)$ should conform to the desired hull form. A properly chosen ellipsoid of revolution would probably suffice.

5.3 CONTROL COEFFICIENTS OF THE TPS

The control coefficients of the tandem propellers are derived below for the case where the TPS operates at a high value of forward velocity, u_0 . (It should be recalled that the control forces for the low speed or hover case can not be expressed independently of the propeller stability forces. Consequently, no analysis of the low-speed control forces is given in this section, since they were treated in Section 5.2.2.2 above, albeit in a preliminary way.)

5.3.1 Evaluation Technique

The propeller forces and moments arising from collective and cyclic pitch control have been derived (using blade-element theory) by the Netherlands Ship Model Basin and presented in Reference (9). The derivation is briefly reviewed here in order to obtain expressions that are consistent with the terminology adopted by CAL and to further account for the different zero reference used by CAL in defining the propeller blade azimuth angle, σ .

Consider the hydrodynamic forces on one blade. Using blade element theory:

* In the absence of experimental data, one should base C_{D1} on the skin friction drag and total surface area, C_{D2} on drag data for cylinders, and C_{D3} on the drag of a flat plate normal to stream direction.

$$L = \frac{1}{2} \rho V^2 C_{L\alpha} \alpha A$$

$$D = \frac{1}{2} \rho V^2 (C_{D0} + f_i C_{L\alpha}^2 \alpha^2) A$$

where V , the blade velocity with respect to the water is given by (see Figure 4-2):

$$V^2 = u_0^2 + \Omega^2 R^2$$

and straight and level flight at high-speed is assumed. Interaction between the propellers is neglected as are inflow velocity and swirl.

The lift and drag forces are first resolved in directions parallel to x and tangent to the average blade circle (in the propeller plane) and then along $x - y - z$ to yield expressions for the propeller control forces. Using the notation and symbols of Figure 4-2 the instantaneous forces/moments, written in propeller axes, are given by:

$$F_x = +/ + \frac{1}{2} \rho V^2 AN \{ C_{L\alpha} \cos \gamma - \sin \gamma [C_{D0} + f_i C_{L\alpha}^2 \alpha^2] \} \quad (5-7)$$

$$|F_T| = \frac{1}{2} \rho V^2 AN \{ C_{L\alpha} \sin \gamma + \cos \gamma [C_{D0} + f_i C_{L\alpha}^2 \alpha^2] \} \quad (5-8)$$

$$F_y = -/+ |F_T| \cos \sigma \quad (5-9)$$

$$F_z = -/+ |F_T| \sin \sigma \quad (5-10)$$

$$M_x = -/+ |F_T| R \quad (5-11)$$

$$M_y = -/- F_x R \cos \sigma \quad (5-12)$$

$$M_z = -/- F_x R \sin \sigma \quad (5-13)$$

in which the notation $-/+$ designates the sign of the term according to whether the propeller in question is forward/aft, and F_x and $|F_T|$ are the lift and drag resolved along x and tangent to the average radius R . As in the case of the stability forces in 5.2.1.2.3, balanced operation is assumed. If this is not the case, differences between the forward and aft propeller, must be taken into account in (5-7) thru (5-13).

By substituting (5-7) or (5-8) into (5-9), (5-10), (5-11), (5-12), and (5-13), letting $\alpha = b_0 + \delta_1 \sin \sigma + \delta_2 \cos \sigma$, and integrating over one cycle with respect to the propeller angle σ , the equations defining the average forces/moments can be written in body axes as:

$$\begin{aligned}
 X: \quad X_C &= \frac{1}{4} \frac{1}{2} \rho V^2 AN \left\{ C_{L_2} \cos \gamma b_0 - \sin \gamma \left[C_{D_0} + f_i C_{L_2}^2 \left\{ b_0^2 + \frac{\delta_1^2 + \delta_2^2}{2} \right\} \right] \right\} \\
 Y: \quad Y_C &= \frac{1}{4} \frac{1}{2} \rho V^2 AN \left\{ C_{L_2} \frac{1}{2} \sin \gamma + \cos \gamma f_i C_{L_2}^2 b_0 \right\} \delta_2 \\
 Z: \quad Z_C &= \frac{1}{4} \frac{1}{2} \rho V^2 AN \left\{ C_{L_2} \frac{1}{2} \sin \gamma + \cos \gamma f_i C_{L_2}^2 b_0 \right\} \delta_1 \\
 K: \quad K_C &= \frac{1}{4} \frac{1}{2} \rho V^2 AN R \left\{ C_{L_2} \sin \gamma b_0 + \cos \gamma \left[C_{D_0} + f_i C_{L_2}^2 \left\{ b_0^2 + \frac{\delta_1^2 + \delta_2^2}{2} \right\} \right] \right\} \\
 M: \quad M_C &= \frac{1}{4} \frac{1}{2} \rho V^2 AN R \left\{ C_{L_2} \frac{1}{2} \cos \gamma - \sin \gamma f_i C_{L_2}^2 b_0 \right\} \delta_2 \quad \frac{1}{4} Z_C l_2 \\
 N: \quad N_C &= \frac{1}{4} \frac{1}{2} \rho V^2 AN R \left\{ C_{L_2} \frac{1}{2} \cos \gamma - \sin \gamma f_i C_{L_2}^2 b_0 \right\} \delta_1 \quad \frac{1}{4} Y_C l_2
 \end{aligned}
 \tag{5-14}$$

Some interesting properties of the cyclicly pitched propeller can be seen from Equations (5-14). In particular, attention is called to the following:

- (1) Thrust is derived primarily from collective pitch, but is diminished by the profile drag term $\sin \gamma C_{D_0}$ and the induced drag term $\sin \gamma f_1 C_x^2 \left\{ b_0^2 + \frac{\delta_1^2 + \delta_2^2}{2} \right\}$. The latter is a function of collective pitch b_0 and cyclic pitch δ_1 and δ_2 .
- (2) Y force is obtained by applying cosine cyclic pitch (δ_2) but is dependent also upon the level of collective pitch (b_0). (A similar remark holds true for Z force).
- (3) The forward (clockwise) propeller produces a negative roll-moment which, for balanced operation, is cancelled by a positive roll-moment due to the (counterclockwise) aft propeller. As in the case of thrust, there is a coupled roll-moment due to cyclic pitch. Notice also, that since the coupled moment is due to induced drag it is independent of the signs of δ_1 and δ_2 .
- (4) The pitch and yaw moments M_c and N_c contain pure couples, generated at the propellers (as indicated by Equations (5-12) and (5-13) and due to the fact that F_x is not axial), as well as moments generated by the propeller forces Z_c and Y_c . As will be seen later these pure couples are small relative to the terms $Z_c l_2$ and $Y_c l_2$.

5.3.2 Reduction to Coefficient Form

The control forces and moments given by the set of Equations (5-14) can be reduced to coefficient form to facilitate the ensuing stability and control investigation. The eventual numerical evaluation of these coefficients will demonstrate, in part, the extent to which the various control cross couplings are significant.

A more conclusive answer to what degree these cross-couplings are significant is obtained from the simulation study discussed in Section VII.

In Equations (5-14) let $b_0 = \delta_0 + \Delta\delta - \gamma_0$, i. e., the angle of attack due to collective pitch is equal to the trim collective pitch, δ_0 , plus the change in collective pitch, $\Delta\delta$, minus the trim flight path angle of the propeller blade, γ_0 . Next, perform a partial differentiation of Equations (5-14) with respect to each of the control inputs $\Delta\delta$, δ_1 , and δ_2 . The method is illustrated below by differentiating the equation for the X control force and defining the resulting coefficients. (The coefficients resulting from differentiating the remaining five equations will be tabulated without discussion).

On letting $b_c = \delta_0 + \Delta\delta - \gamma_0$, the basic expression for thrust of the forward propeller is:

$$X_c = \frac{1}{2} \rho V^2 AN \left\{ C_{L_x} \cos \gamma_0 [\delta_0 + \Delta\delta - \gamma_0] - \sin \gamma_0 \left[C_{D_0} + f_1 C_{L_x}^2 \cdot \left\{ (\delta_0 + \Delta\delta - \gamma_0)^2 + \frac{\delta_1^2 + \delta_2^2}{2} \right\} \right] \right\}$$

Noting that $V^2 = u_0^2 / \sin^2 \gamma_0$, X_c becomes:

$$X_c = \frac{1}{2} \rho \frac{u_0^2 AN}{\sin^2 \gamma_0} \left\{ C_{L_x} \cot \gamma_0 [\delta_0 + \Delta\delta - \gamma_0] - C_{D_0} - f_1 C_{L_x}^2 \cdot \left[(\delta_0 + \Delta\delta - \gamma_0)^2 + \frac{\delta_1^2 + \delta_2^2}{2} \right] \right\}$$

Letting

$$\frac{\partial (X_c)}{\partial (\Delta\delta)} = X_{\Delta\delta} \quad ; \quad 2 \frac{\partial (X_c)}{\partial (\Delta\delta)^2} = X_{(\Delta\delta)^2}$$

$$\frac{\partial (X_c)}{\partial (\delta_1^2)} = X_{\delta_1^2} \quad ; \quad \frac{\partial (X_c)}{\partial (\delta_2^2)} = X_{\delta_2^2}$$

and taking the partial derivatives indicated, the γ -force coefficients become (after the substitution $\alpha_0 = \delta_0 \cdot \gamma_0$ is made):

$$X_{\Delta\delta} = \frac{1}{2} \rho \frac{u_0^2 AN}{\sin \gamma_0} \left\{ C_{L\alpha} \cot \gamma_0 - 2 f_1 C_{L\alpha}^2 \alpha_0 \right\}$$

$$X_{(\Delta\delta)^2} = -\frac{1}{2} \rho \frac{u_0^2 AN}{\sin \gamma_0} \left\{ 2 f_1 C_{L\alpha}^2 \right\}$$

$$X_{\delta_1^2} = -\frac{1}{2} \rho \frac{u_0^2 AN}{\sin \gamma_0} \left\{ \frac{1}{2} f_1 C_{L\alpha}^2 \right\}$$

$$X_{\delta_2^2} = -\frac{1}{2} \rho \frac{u_0^2 AN}{\sin \gamma_0} \left\{ \frac{1}{2} f_1 C_{L\alpha}^2 \right\}$$

For simplicity, let

$$X_{\delta_1^2} = X_{\delta_2^2} = X_{\delta^2} = -\frac{1}{2} \rho \frac{u_0^2 AN}{\sin \gamma_0} \left\{ \frac{1}{2} f_1 C_{L\alpha}^2 \right\}$$

The force and moment coefficients for the remaining axes can be arrived at in the same way. These are listed below (for the forward propeller):

$$Y_{\delta} = \frac{\partial(\gamma_c)}{\partial(\delta_2)} = -\frac{1}{2} \rho \frac{u_0^2 AN}{\sin \gamma_0} \left\{ \frac{1}{2} C_{L\alpha} + \cot \gamma_0 f_1 C_{L\alpha}^2 \alpha_0 \right\}$$

$$Y_{\Delta\delta\cdot\delta} = \frac{\partial(Y_c)}{\partial(\Delta\delta\cdot\delta_2)} = -\frac{1}{2}\rho \frac{u_0^2 AN}{\sin \gamma_0} \left\{ \cot \gamma_0 f_1 C_{L\alpha}^2 \right\}$$

$$Z_\delta = \frac{\partial(Z_c)}{\partial(\delta_1)} = Y_\delta$$

$$Z_{\Delta\delta\cdot\delta} = \frac{\partial(Z_c)}{\partial(\Delta\delta\cdot\delta_1)} = Y_{\Delta\delta\cdot\delta}$$

$$K_{\Delta\delta} = \frac{\partial(K_c)}{\partial(\Delta\delta)} = -\frac{1}{2}\rho \frac{u_0^2 ANR}{\sin \gamma_0} \left\{ C_{L\alpha} + 2 \cot \gamma_0 f_1 C_{L\alpha}^2 \alpha_0 \right\}$$

$$K_{\delta^2} = \frac{\partial(K_c)}{\partial(\delta_1^2 \text{ or } \delta_2^2)} = -\frac{1}{2}\rho \frac{u_0^2 ANR}{\sin \gamma_0} \left\{ \frac{1}{2} \cot \gamma_0 f_1 C_{L\alpha}^2 \right\}$$

$$K_{(\Delta\delta)^2} = \frac{\partial(K_c)}{\partial(\Delta\delta)^2} = -\frac{1}{2}\rho \frac{u_0^2 ANR}{\sin \gamma_0} \left\{ 2 \cot \gamma_0 f_1 C_{L\alpha}^2 \right\}$$

$$M_\delta = \frac{\partial(M_c)}{\partial(\delta_1)} = -Z_\delta l_2$$

$$M_{\delta_2} = \frac{\partial(M_c)}{\partial(\delta_2)} = -\frac{1}{2}\rho \frac{u_0^2 ANR}{\sin \gamma_0} \left\{ \frac{1}{2} C_{L\alpha} \cot \gamma_0 - f_1 C_{L\alpha}^2 \alpha_0 \right\}$$

$$M_{\Delta\delta\cdot\delta_2} = \frac{\partial(M_c)}{\partial(\Delta\delta\cdot\delta_2)} = \frac{1}{2}\rho \frac{u_0^2 ANR}{\sin \gamma_0} \left\{ f_1 C_{L\alpha}^2 \right\}$$

$$N_{\delta} = \frac{\partial(N_C)}{\partial(\delta_2)} = Y_{\delta} l_2$$

$$N_{\delta_1} = \frac{\partial(N_C)}{\partial(\delta_1)} = M_{\delta_2}$$

$$N_{\Delta\delta \cdot \delta_1} = \frac{\partial(N_C)}{\partial(\Delta\delta \cdot \delta_1)} = M_{\Delta\delta \cdot \delta_2}$$

Using the above force/moment coefficients the following set of control force/moment equations result. Balanced operation is assumed, with forward propeller and aft propeller coefficients being equal in magnitude.

$$X_C = F_{x_0} + X_{\Delta\delta} (\Delta\delta_f + \Delta\delta_a) + X_{\Delta\delta^2} (\Delta\delta_f^2 + \Delta\delta_a^2) + X_{\delta^2} (\delta_{1f}^2 + \delta_{1a}^2 + \delta_{2f}^2 + \delta_{2a}^2)$$

$$\begin{aligned}
Y_C &= Y_\delta (\delta_{2f} - \delta_{2a}) + Y_{\Delta\delta \cdot \delta} (\Delta\delta_f \delta_{2f} - \Delta\delta_a \delta_{2a}) \\
Z_C &= Z_\delta (\delta_{1f} - \delta_{1a}) + Z_{\Delta\delta \cdot \delta} (\Delta\delta_f \delta_{1f} - \Delta\delta_a \delta_{1a}) \\
K_C &= K_{\Delta\delta} (\Delta\delta_f - \Delta\delta_a) + K_{\Delta\delta^2} (\Delta\delta_f^2 - \Delta\delta_a^2) + K_{\delta^2} (\delta_{1f}^2 - \delta_{1a}^2 + \delta_{2f}^2 - \delta_{2a}^2) \\
M_C &= M_\delta (\delta_{1f} + \delta_{1a}) - Z_{\Delta\delta \cdot \delta} L_z (\Delta\delta_f \delta_{1f} + \Delta\delta_a \delta_{1a}) + M_{\delta_2} (\delta_{2f} + \delta_{2a}) \\
&\quad + M_{\Delta\delta \cdot \delta_2} (\Delta\delta_f \delta_{2f} + \Delta\delta_a \delta_{2a}) \\
N_C &= N_\delta (\delta_{2f} + \delta_{2a}) + Y_{\Delta\delta \cdot \delta} L_z (\Delta\delta_f \delta_{2f} + \Delta\delta_a \delta_{2a}) + N_{\delta_1} (\delta_{1f} + \delta_{1a}) + N_{\Delta\delta \cdot \delta_1} (\Delta\delta_f \delta_{1f} + \Delta\delta_a \delta_{1a})
\end{aligned}
\tag{5-15}$$

Notice that except for the trim thrust F_{T_0} (the trim moments cancel for balanced operation) the above set of equations describe perturbation forces/moments since, if $\Delta\delta = \delta_1 = \delta_2 = 0$, they reduce to zero.

If the trim term in (5-15) is ignored for the moment, the control forces and moments are seen to consist of a set of primary control terms and a set of cross-coupled or cross-axis terms. Let the control inputs, forward and aft, be defined in the following way:

$$\begin{aligned}
x\text{-axis (force) control input} &= \delta_x = \Delta\delta_f + \Delta\delta_a \\
y\text{-axis (force) control input} &= \delta_y = \delta_{2f} - \delta_{2a} \\
z\text{-axis (force) control input} &= \delta_z = \delta_{1f} - \delta_{1a} \\
x\text{-axis (moment) control input} &= \delta_K = \Delta\delta_f - \Delta\delta_a \\
y\text{-axis (moment) control input} &= \delta_M = \delta_{1f} + \delta_{1a} \\
z\text{-axis (moment) control input} &= \delta_N = \delta_{2f} + \delta_{2a}
\end{aligned}
\tag{5-16}$$

The primary control terms are then:

$$\begin{aligned}
X: & X_{\Delta S} \delta_X \\
Y: & Y_{\delta} \delta_Y \\
Z: & Z_{\delta} \delta_Z \\
K: & K_{\Delta S} \delta_K \\
M: & M_{\delta} \delta_M \\
N: & N_{\delta} \delta_N
\end{aligned}
\tag{5-17}$$

and the undesirable cross-coupling terms are:

$$\begin{aligned}
X: & \frac{1}{2} X_{\Delta S}^2 (\delta_X^2 + \delta_K^2) + \frac{1}{2} X_{\delta}^2 (\delta_Y^2 + \delta_Z^2 + \delta_M^2 + \delta_N^2) \\
Y: & \frac{1}{2} Y_{\Delta S \cdot \delta} (\delta_X \delta_Y + \delta_K \delta_N) \\
Z: & \frac{1}{2} Z_{\Delta S \cdot \delta} (\delta_X \delta_Z + \delta_K \delta_M) \\
K: & K_{\Delta S}^2 (\delta_X \delta_K) + K_{\delta}^2 (\delta_Z \delta_M + \delta_Y \delta_N) \\
M: & -\frac{1}{2} Z_{\Delta S \cdot \delta} l_2 (\delta_X \delta_M + \delta_K \delta_Z) + M_{\delta_2} (\delta_N) + M_{\Delta S \cdot \delta_2} (\delta_X \delta_N + \delta_K \delta_Y) \\
N: & \frac{1}{2} Y_{\Delta S \cdot \delta} l_2 (\delta_X \delta_N + \delta_K \delta_Y) + N_{\delta_2} (\delta_M) + N_{\Delta S \cdot \delta_1} (\delta_X \delta_M + \delta_K \delta_Z)
\end{aligned}
\tag{5-18}$$

Notice that most of the coupling terms are non-linear, since they involve the squares and products of the control inputs.

5.4 ADDED-MASS COEFFICIENTS

For the purposes of this study, the moments of inertia of the TPS were computed by assuming the submarine to be a homogeneous ellipsoid of revolution. The coefficients of apparent mass and inertia were derived from classical sources in the literature, again assuming the submarine to be a prolate ellipsoid. The numerical results are tabulated in Table 6-1, where the terminology employed for defining the real and "added" masses and inertias is that established by SNAME.

VI

EQUILIBRIUM EQUATIONS AND NUMERICAL DATA

6.1 THE SIX-DEGREE-OF-FREEDOM EQUATIONS OF MOTION

In Section V the propeller and hull hydrodynamic forces/moments were written in perturbation form using dimensional derivatives which incorporated both the hull and the propeller effects. These forces and moments were defined as: ΣX , ΣY , ΣZ , ΣK , ΣM , ΣN . The propeller propulsion and control forces/moments were also discussed in Section V and designated X_c , Y_c , Z_c , K_c , M_c , N_c . If the gyroscopic terms are added to these two groups of body forces/moments and the results are equated to the mass/inertia reaction terms, the complete six-degree-of-freedom equations of motion, in abbreviated form, become:

$$\begin{aligned}
 X: \quad & m_1 \dot{u} - m_2 r v + m_3 q w = \Sigma X + X_c \\
 Y: \quad & m_2 \dot{v} + m_1 r u - m_3 p w = \Sigma Y + Y_c \\
 Z: \quad & m_3 \dot{w} - m_1 q u + m_2 p v = \Sigma Z + Z_c \\
 K: \quad & I_{xx} \dot{p} + (I_{zz} - I_{yy}) q r = \Sigma K + K_c \\
 M: \quad & I_{yy} \dot{q} + (I_{xx} - I_{zz}) p r = -(H_f - H_a) r + \Sigma M + M_c \\
 N: \quad & I_{zz} \dot{r} + (I_{yy} - I_{xx}) p q = (H_f - H_a) q + \Sigma N + N_c
 \end{aligned} \tag{6-1}$$

In 6-1, H_f and H_a are the forward and aft propeller angular momenta, giving rise to the gyroscopic moments indicated. These moments are zero if the forward and aft propeller speeds are the same and the effective polar moments of inertia are equal. Note that as a consequence of the assumption that the submarine is a body of revolution, the $x - y - z$ axes are principle axes and all products of inertia are zero.

6.2 TRIM CONDITIONS - TWO PROPELLERS OPERATING

Using the set of equations which define the control forces/moments (Eq. 5-14) and letting the cyclic pitch components (δ_1 and δ_2) and the change in collective pitch ($\Delta \delta$) be zero, the trim equations result: (the notation $+/-$ designates the sign for the forward/aft propellers)

$$F_{x0} = X_{c0} = \pm \frac{1}{2} \rho V^2 AN \{ C_{L\alpha} \cos \gamma_0 \alpha_0 - \sin \gamma_0 [C_{d0} + f_1 C_{L\alpha}^2 \alpha_0^2] \} \tag{6-2}$$

$$M_{x0} = K_{c0} = \pm \frac{1}{2} \rho V^2 ANR \{ C_{L\alpha} \sin \gamma_0 \alpha_0 + \cos \gamma_0 [C_{d0} + f_1 C_{L\alpha}^2 \alpha_0^2] \} \tag{6-3}$$

$$P_0 = |M_{x0}| \Omega, \text{ per propeller} \tag{6-4}$$

Note that, in straight and level flight, all other components of control force/moment are zero.

In order to establish the trim conditions for the high-speed case, expression 6-2 is equated to the hull drag. Thus, for balanced operation of the propellers:

$$\frac{1}{2} \rho V^2 A_p C_{L_x} \cos \gamma_0 d_0 - \sin \gamma_0 [C_{D_0} + f_i C_{L_x}^2 d_0^2] = \frac{1}{2} \rho L^2 u_0^2 X'_H \quad (6-5)$$

A parametric investigation of the effects of the variables γ_0 , d_0 , N , A on propulsion efficiency and other performance factors would ordinarily be made in a comprehensive design study. However, no such study was made in the present program. Instead, the value of N suggested by Electric Boat, Reference (10), was used and a blade of reasonable size was chosen on the basis of rough horsepower calculations. If the angle of attack corresponding to maximum lift/drag is inserted into equation (6-5) a solution for γ_0 is obtained. Forward speed and horsepower then become direct functions of propeller speed Ω . Thus with:

$$N = 16$$

$$A = 3 \text{ ft}^2$$

$$\alpha_0 = .10 \text{ rad (max } L/D \text{)}$$

$$\gamma_0 \approx 35^\circ$$

and propeller speed = 50 rpm, the forward speed and horsepower are:

$$u_0 = 40.4 \text{ FT/sec (24 knots)}$$

$$P_0 \approx 5740 \text{ hp per propeller.}$$

Based on these trim conditions the parameters needed in the computation of the propeller derivatives of 6.4 below are:

$$\begin{aligned}
 F_{x0} &\approx +/4 \quad 66,100\# \\
 M_{x0} &\approx -/4 \quad 601,000\# \text{ ft} \\
 \lambda_T &= -/4 \quad 2.20 \\
 \lambda_\phi &= -/4 \quad 1.75 \\
 k_z &= +/4 \quad .211
 \end{aligned}$$

The above set of constants were used in all of the high-speed stability and control work to be described in Section VII.

6.3 TRIM CONDITIONS - ONE PROPELLER OPERATING

Under certain operational conditions it may be necessary or desirable to operate the TPS with one propeller running and the other one locked. The results of a brief investigation of the required trim settings for this mode of operation are described below.

The following principal assumptions were made:

- (1) The forward propeller is rotating in a trimmed condition at some blade flight path angle γ_f and angle-of-attack α_f corresponding to trim pitch δ_{of} ($\Delta\delta_f$, δ_{1f} and δ_{2f} are zero). The submarine is in straight and level flight.
- (2) The aft propeller is locked with the blades set at some angle of attack α_a , γ_a being $+\pi/2$.
- (3) The lift curve slopes for the forward and aft propellers are the same (i. e., the cascade effects are the same).

The conditions to be met are (a) net thrust = total drag and (b) the sum of the X -moments = zero. Using equations 6-2 and 6-3 these constraints can be expressed as:

$$\frac{1}{2} \rho V^2 AN \{ C_{L\alpha} \alpha_f \cos \gamma_f - \sin \gamma_f (C_{d_0} + f_1 C_{L\alpha}^2 \alpha_f^2) \} \quad (6-6)$$

$$= \frac{1}{2} \rho l^2 \chi' u u_0^2 + \frac{1}{2} \rho u_0^2 AN (C_{d_0} + f_1 C_{L\alpha}^2 \alpha_a^2)$$

in which the hull drag derivative is assumed to be valid at the total speed u_0 , and

$$-\frac{1}{2} \rho V^2 AN R \{ C_{L\alpha} \alpha_f \sin \gamma_f + \cos \gamma_f [C_{d_0} + f_1 C_{L\alpha}^2 \alpha_f^2] \} \quad (6-7)$$

$$+ \frac{1}{2} \rho u_0^2 AN R C_{L\alpha} \alpha_a = 0$$

Expression 6-7 can be solved for the aft angle-of-attack:

$$\alpha_a = \left(\frac{V}{u_0} \right)^2 \frac{C_{L\alpha} \alpha_f \sin \gamma_f + \cos \gamma_f (C_{d_0} + f_1 C_{L\alpha}^2 \alpha_f^2)}{C_{L\alpha}} \quad (6-8)$$

which is seen to be a function of γ_f and α_f only ($V/u_0 = \text{cosec } \gamma_f$) and not directly dependent on the speed parameters (Ω or u_0). For any particular set of values γ_f and α_f , α_a is found from 6-8.

If the expression for α_a given by 6-8 is substituted into the thrust-drag equation 6-6 a quartic equation in the variable α_f can be written, in which the coefficients are functions of γ_f and the physical constants of the system. This equation, 6-9, will contain within it the thrust-drag constraint as well as the moment balance constraint. The expression is:

$$\chi^4 + A \chi^3 + B \chi^2 + C \chi + D = 0 \quad (6-9)$$

where

$$\chi = f_1 C_{L\alpha} \alpha_f$$

and

$$A = 2 \tan \gamma_f$$

$$B = \tan^2 \gamma_f (1 + \sin \gamma_f) + 2 f_1 C_{d_0}$$

$$C = \tan \gamma_f (2 C_{d_0} f_1 - \sin \gamma_f)$$

$$D = f_1 (\sin \gamma_f \tan \gamma_f)^2 \left\{ \frac{l^2 \chi' u}{AN} + C_{d_0} \left(\frac{1 + \sin \gamma_f}{\sin \gamma_f} \right) \right\} + (f_1 C_{d_0})^2$$

Equation (6-9) was solved for various values of δ_f between 5° and 30° . The values of α_f which are physically realizable* and which correspond to these δ_f are plotted in Figure 6-1. Also shown in the figure are the corresponding settings of the aft propeller, found from equation (6-8).

Having determined the permissible set of δ_f and α_f which will satisfy the thrust-drag equality, and the corresponding α_a needed to achieve roll-moment balance, it is necessary to next consider forward propeller power. The forward propeller power is:

$$P_{of} = M_{Aof} \Omega = P_o (P_{oa} = 0) \quad (6-10)$$

Using equation 6-3 and on nondimensionalizing (6-10) by dividing by $\frac{1}{2} \rho A N U_o^3$ one obtains a nondimensional power equation:

$$P = \frac{P_o}{\frac{1}{2} \rho A N U_o^3} = \frac{C_L c_d \alpha_f \sin \delta_f + \cos \delta_f [C_{d_o} + f_i C_{L^2} \alpha_f^2]}{\tan \delta_f \sin^2 \delta_f} \quad (6-11)$$

In Figure 6-2 P is plotted versus δ_f , the forward propeller (blade) flight-path-angle. A minimum occurs around 23° , corresponding to α_f of about 4.8° and α_a of about 14.7° .

In order to observe the trend in the variation among the variables V_o (forward speed), Ω (propeller angular velocity) and horsepower, two sets of calculations were made: one at variable δ_f and max Ω (50 rpm), and one at constant δ_f and variable Ω . The forward speed is common to both sets of calculations. The results (approximate) are:

* Extraneous values arise from the squaring operation involved in eliminating α_a and neglect of the absolute value limitation on the induced drag for the angle range considered.

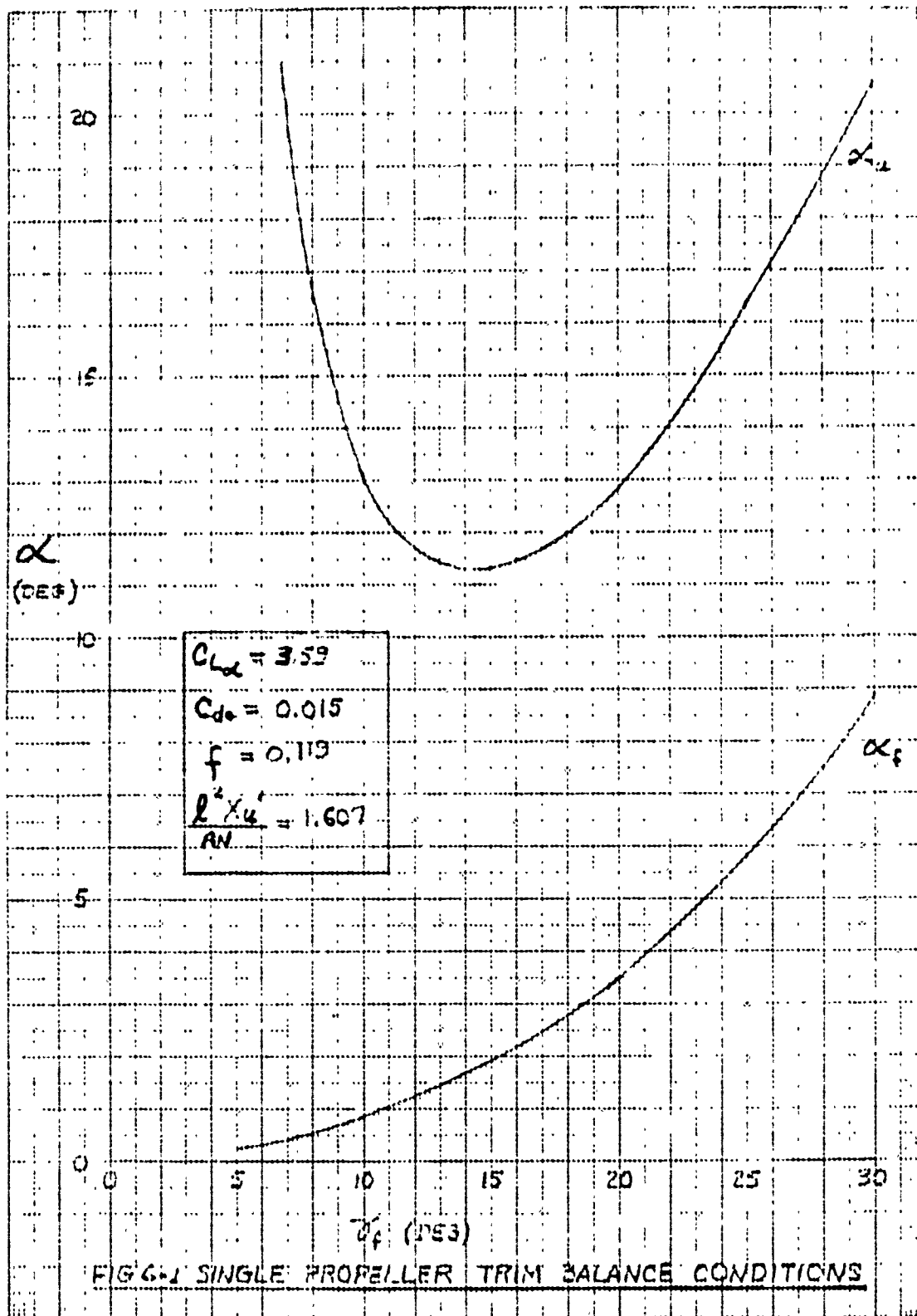


FIGURE 6-1 Single Propeller Trim Balance Conditions

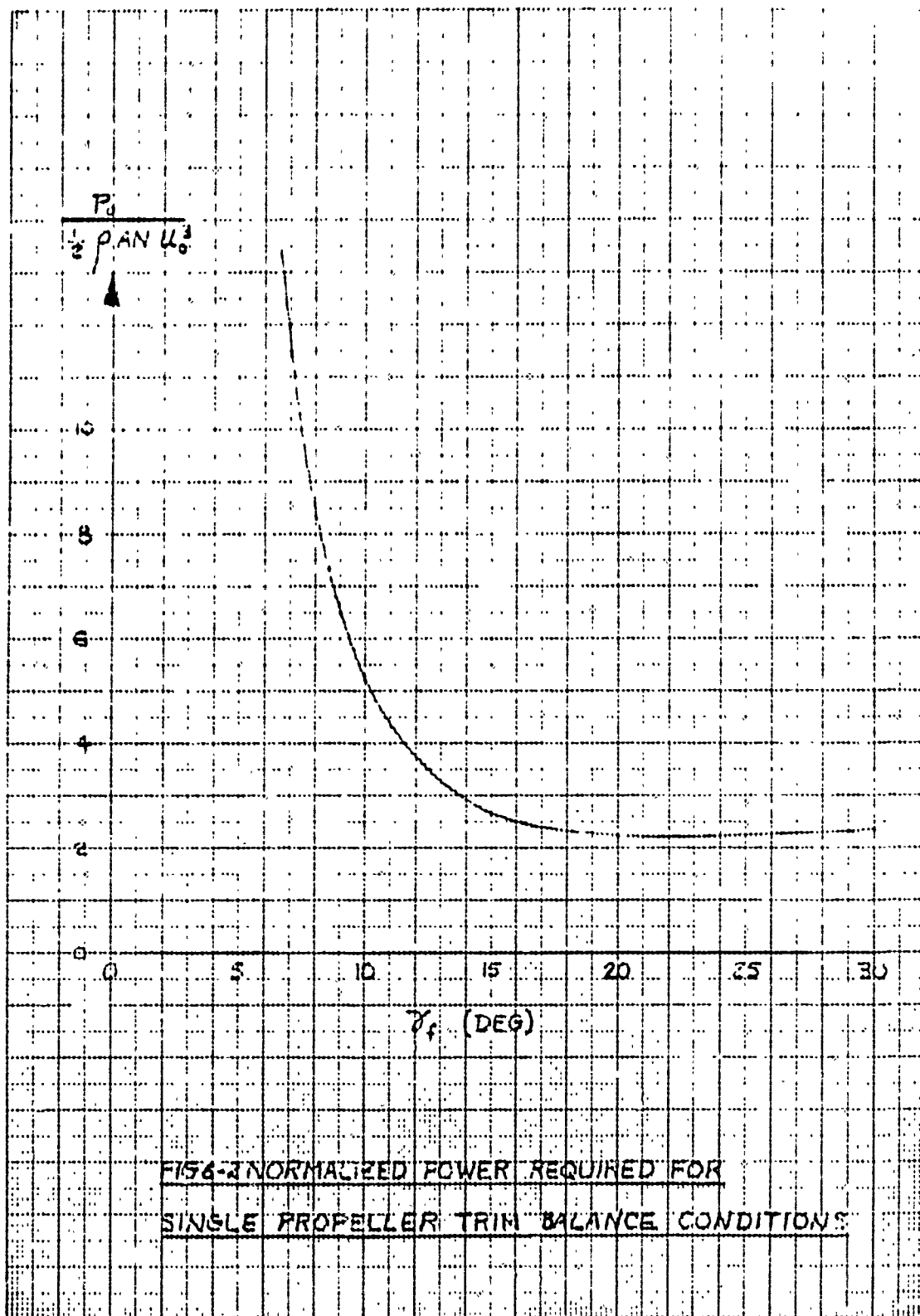


FIGURE 6-2 Normalized Power Required for Single Propeller Trim Balance Condition.

U_0 ft/sec.	Constant (max) Ω , 50 rpm			Constant δ_f			
	δ_f	P_{HP}	U_0/P_{HP}	δ_f	P_{HP}	U_0/P_{HP}	rpm
10.16	10°	478	.021	23°	202	.050	20.8
15.5	15°	882	.018	23°	720	.022	31.7
24.5	23°	2820	.0087	23°	2820	.0087	50
27	25°	3780	.0072	requires rpm > 50			

Figure 6-2 shows that in order to operate at maximum U_0/P_{HP} (minimum P_0/U_0^3) at all speeds, a δ_f in the vicinity of 22 or 23 degrees should be used, and this is borne out by the tabulated data. Since $\delta_f = 23^\circ$ corresponds to $\alpha_f = 4.8^\circ$ and, since the δ_f corresponding to α_f (max L/D)^{*} is closer to 25°, the question arose as to whether computational inaccuracies may have crept into Fig. 6-2 to mask a minimum closer to 25°. However, a check of the computations used in this figure indicates otherwise. Apparently then, optimum operation does not occur at α_f (max L/D).

Aside from any question as to what are the exact optimum operating conditions, it is obvious from the above computations, that operation with one propeller locked is practical and that speeds of about 27 ft/sec (16 knots) are possible.

6.4 NUMERICAL DATA

All of the numerical data used in connection with the stability and control studies are collected in this section.

6.4.1 Physical Data

Physical data for the hull and the propellers as well as trim parameters for balanced two-propeller operation are given in Table 6-1 for the high-speed case.

* α_f (max L/D) = 5.7°

TABLE 6-1
PHYSICAL DATA

$W = 9.63 \times 10^6 \#$	$l_1 = 12.5'$	$f = 8.6$
$\Delta = 4300 \text{ LONG TONS}$	$l_2 = 110' (\text{FWD. \& AFT})$	$m = 299.3 \times 10^3 \text{ SLUGS}$
$l = 275'$	$d = 32'$	$M_\theta = -9.63 \times 10^6 \text{ ft.}^\# / \text{rad.}$
		$z_b = -1.0 \text{ ft.}$

$$m_1 = m(1+K_1) = m(1.026) = 307.1 \times 10^3$$

$$m_2 = m(1+K_2) = m(1.95) = 583.7 \times 10^3$$

$$m_3 = m(1+K_3) = m(1.95) = 583.7 \times 10^3$$

$$I_{x0} = ml^2/10f^2 = 30.61 \times 10^6 \# \text{ ft.} \cdot \text{sec}^2$$

$$I_{y0} = m(.23l)^2 = 1197 \times 10^6$$

$$I_{z0} = m(.23l)^2 = 1197 \times 10^6$$

$$I_{xx} = I_{x0}(1+K_4) = I_{x0}(1) = 30.61 \times 10^6$$

$$I_{yy} = I_{y0}(1+K_5) = I_{y0}(1.86) = 2227 \times 10^6$$

$$I_{zz} = I_{z0}(1+K_6) = I_{z0}(1.86) = 2227 \times 10^6$$

$C_{d0} = .015$	$V = 70.5'/\text{sec.}$	$\lambda_T = -2.20$
$C_{L\alpha} = 3.59$	$N = 16$	$\lambda_Q = -1.75$
$f_1 = .119$	$A = 3 \text{ ft}^2$	$k_2 = .211$
$\alpha_0 = .10 \text{ rad.}$	$R = 11'$	$F_{x0} \cong 66,100 \#/\text{prop.}$
$\Omega = 5.25 \text{ rad}/\text{sec.} (-50 \text{ RPM})$	$D = 22'$	$M_{x0} \cong 601,000 \text{ ft}^\#/\text{prop.}$
$\delta_0 \cong 35^\circ$	$u_0 = 40.4'/\text{sec.} (24 \text{ knots})$	$P_0 \cong 5740 \text{ hp}/\text{prop.}$

TABLE 6-1 - Physical Data

6.4.2 Hull and Propeller Hydrodynamics

The non-dimensional stability derivatives for the hull (X'_u, Y'_v , etc.) and the dimensional derivatives for the propellers (X_u^p, Y_v^p , etc.) are not listed separately. Instead, these derivatives are listed together, in Table 6-2 where their combined effect is accounted for by the "total" stability derivatives (X_u, Y_v , etc.) noted earlier in Section V. In Table 6-2 the relative effect of each contribution, hull and propeller, can be noted and their sum compared with the corresponding derivatives of a conventional submarine. The particular conventional submarine for which data were available at the time of writing this report, is the Albacore, although eventually it is hoped that comparison with a submarine of the Thresher class will be possible.

Most of the values for the hull and propeller derivatives given in Table 6-2 can be passed over without comment. However, there are a few of these derivatives which are worthy of a few remarks.

- (1) Although at high speed the contribution to X_u (rate-of-change-of-drag with change in forward velocity), due to the propellers is much larger than that due to the hull, the relative contribution to total drag at 40.4 FT/sec is: hull drag \approx 132,000#, propeller drag \approx 8100#. The propeller drag, for two propellers operating, can be computed from the negative component of the trim thrust given in equation (6-2).
- (2) The propellers contribute a significant amount of damping in heave (Z_w), over that due to the bare hull, but not enough to match the effect of the empennage in a conventional submarine.
- (3) Although the propellers contribute significantly to damping in pitch ($M_{\dot{\theta}}$) and damping in yaw (N_r) over the bare hull, the contribution is not as effective as the empennage in a conventional submarine.

TOTAL HULL & PROPELLER DERIVATIVES				
DEFINITIONS	HULL CONTRIBUTION	PROPELLER CONTRIBUTION	TOTAL	ALBACORE
$X_u = \frac{1}{2} \rho l^2 U X'_u + \frac{4F_{x0}}{u_0} \lambda_T$	-315×10^3	-14387×10^3	-175×10^3	-161×10^3
$X_v = \frac{1}{2} \rho l^2 U X'_v - \frac{4M_{x0}}{u_0} (1 - \lambda_a)$	-638×10^3	-12408×10^3	-74.2×10^3	-638×10^3
$X_T = \frac{1}{2} \rho l^2 U X'_T$	-1258×10^3		-1258×10^3	$+1937 \times 10^3$
$Y_p = \frac{1}{2} \rho l^2 U Y'_p$	-466×10^3		-466×10^3	-199×10^3
$Z_w = \frac{1}{2} \rho l^2 U Z'_w - \frac{4M_{z0}}{u_0} (1 - \lambda_a)$	-15.15×10^3	-10.406×10^3	-2556×10^3	-34.7×10^3
$Z_g = \frac{1}{2} \rho l^2 U Z'_g$	-555×10^3		-555×10^3	-3163×10^3
$K_v = \frac{1}{2} \rho l^2 U K'_v$	-472×10^3		-472×10^3	-690×10^3
$K_p = \frac{1}{2} \rho l^2 U K'_p - \frac{4M_{x0}}{u_0} (1 - \lambda_a)$	-10.78×10^6	-1.26×10^6	-12.04×10^6	-3.81×10^6
$K_T = \frac{1}{2} \rho l^2 U K'_T$	-285×10^6		-285×10^6	-1397×10^6
$K_u^p = -\frac{2}{u_0} (M_{x0} + M_{x0a}) \lambda_a$				
$M_w = \frac{1}{2} \rho l^2 U M'_w$	$+582 \times 10^6$		$+582 \times 10^6$	$+2021 \times 10^6$
$M_z = \frac{1}{2} \rho l^2 U M'_z + 2k_2 F_{x0} \frac{D^2}{u_0} \lambda_T - \frac{4M_{z0}}{u_0} (1 - \lambda_a) l_2$	-90.2×10^6	$-137 \times 10^6 - 1259 \times 10^6$	-2668×10^6	-2665×10^6
$M_T = -\frac{4F_{x0}}{u_0} (1 - \lambda_T) l_2 - \frac{4M_{z0}}{u_0} \lambda_a l_2$		-12.01×10^6	-12.01×10^6	
$N_v = \frac{1}{2} \rho l^2 U N'_v$	-723×10^6		-723×10^6	-383×10^6
$N_p = \frac{1}{2} \rho l^2 U N'_p$	-2.80×10^6		-2.8×10^6	-5.5×10^6
$N_g = \frac{2M_{z0}}{u_0} \lambda_a l_2 + \frac{4F_{x0}}{u_0} (1 - \lambda_T) l_2$		$+12.01 \times 10^6$	$+12.01 \times 10^6$	
$N_T = \frac{1}{2} \rho l^2 U N'_T - \frac{4M_{z0}}{u_0} (1 - \lambda_a) l_2^2 + 2k_2 F_{x0} \frac{D^2}{u_0} \lambda_T$	-166×10^6	$-126 \times 10^6 - 237 \times 10^6$	-293×10^6	-177×10^6

TABLE 6-2 - Total Hull & Propeller Derivatives

6.4.3 Control Coefficients

The numerical values for the primary control coefficients, along with the corresponding designated control inputs are given in Table 6-3. By way of comparison with a conventional submarine, the Albacore z -force coefficient (Z_g) is about three times as large, and the pitching moment coefficient (M_g) about four times as large as the values in Table 6-3.

The control cross-coupling coefficients are listed in Table 6-4. The effect of these cross-coupling coefficients on control system performance will be discussed in Section VII.

TABLE 6-3			
PRIMARY CONTROL COEFFICIENTS			
AXIS	CONTROL INPUT	COEFFICIENT	VALUE
X	δ_x	$X_{\Delta\delta}$	$660 \times 10^3 \#/\text{rad.}$
Y	δ_y	Y_{δ}	$-275 \times 10^3 \#/\text{rad.}$
Z	δ_z	Z_{δ}	$-275 \times 10^3 \#/\text{rad.}$
X	δ_K	$K_{\Delta\delta}$	$-6.066 \times 10^6 \text{ ft}^2/\text{rad.}$
Y	δ_M	$-Z_{\delta} l_2 = M_{\delta}$	$+30.25 \times 10^6 \text{ ft}^2/\text{rad.}$
Z	δ_N	$Y_{\delta} l_2 = N_{\delta}$	$-30.25 \times 10^6 \text{ ft}^2/\text{rad.}$

TABLE 6-4			
CONTROL COUPLING COEFFICIENTS			
COEFFICIENT	VALUE	COEFF'T.	VALUE
$X(\Delta\delta)^2$	$-420 \times 10^3 \#/\text{rad.}^2$	M_{δ_2}	$-3.6 \times 10^6 \# \text{ ft}^2/\text{rad.}$
X_{δ^2}	$-105 \times 10^3 \#/\text{rad.}^2$	$M_{\Delta\delta\delta_2}$	$+1.6 \times 10^6 \# \text{ ft}^2/\text{rad.}^2$
$Y_{\Delta\delta\delta}$	$-300 \times 10^3 \#/\text{rad.}^2$	$Y_{\Delta\delta\delta} l_2$	$-33.00 \times 10^6 \# \text{ ft}^2/\text{rad.}^2$
$Z_{\Delta\delta\delta}$	$-300 \times 10^3 \#/\text{rad.}^2$	N_{δ_1}	$-36 \times 10^6 \# \text{ ft}^2/\text{rad.}$
$K(\Delta\delta)^2$	$-6.600 \times 10^6 \text{ ft}^2/\text{rad.}^2$	$N_{\Delta\delta\delta_1}$	$+1.16 \times 10^6 \# \text{ ft}^2/\text{rad.}^2$
K_{δ^2}	$-1.650 \times 10^6 \text{ ft}^2/\text{rad.}^2$		
$Z_{\Delta\delta\delta} l_2$	$-33.00 \times 10^6 \text{ ft}^2/\text{rad.}^2$		

TABLE 6-3 - Primary Control Coefficients
 TABLE 6-4 - Control Coupling Coefficients

VII

STABILITY AND CONTROL STUDIES

7.1 GENERAL REMARKS

The stability and control properties of the TPS are an essential element of the total number of factors that bear on the engineering feasibility of the TPS concept. In the most general sense, the concept under investigation postulates a control configuration that has greater control effectiveness at low (or zero) speed, plus greater flexibility in producing control forces and moments at all speeds, than a conventional submarine. This gain in control capability is also accompanied by a loss in dynamic stability (including a loss in control effectiveness at high speeds) as a result of the elimination of the stabilizing surfaces (fixed planes and fins) found on the conventional submarine. This means that the TPS will not reach any attitude, depth, or heading trim when proceeding forward at high speeds unless the hydrodynamic forces and moments that cause the submarine to diverge from the intended path are continually corrected or counter-balanced by control-force and moment inputs.

This continual correction task can be done either manually by a human controller or by an automatic control system. If the stabilization task is undertaken by the human operator, in addition to his maneuver-control task, the magnitude and difficulty of this task enters into the assessment of the handling

qualities of the submarine. Although it may be possible to stabilize and control the TPS by manual means, the extent to which a human operator(s) could do this in acceptable fashion is open to question. A glance at the response of the unmodified (i. e., operated open loop) TPS (see Figure (7-1)) shows that when $U_0 = 40$ ft/sec., the pitch angle, θ , diverges about 15 degrees in about 15 seconds. Accordingly, a basic premise in this stability and control investigation is that automatic-stabilization methods must be employed.

The need to employ control forces and moments for stabilization purposes immediately poses the question as to what extent the stabilization function, whether done manually or automatically, will detract from the maneuverability of the TPS. If part of the available control power must be used to offset the existing destabilizing hydrodynamic forces, then the total available control power can not be used for maneuvering purposes. In essence, this is the central issue of feasibility from the stability and control point of view, namely, to what extent does maneuverability suffer from the requirement to stabilize with the control function. Of course, there are secondary stability and control questions, e. g., to what extent are problems created by the pitch-yaw and yaw-pitch couplings that are present in the cyclic-pitch control process.

The major purpose of this initial feasibility investigation is to resolve this central issue of stabilization versus maneuverability and to consider, where possible, all those characteristics of tandem-propeller control that have a bearing on the feasibility of designing an actual control system. The overall task remains to be completed within the time period of the existing contract. To date, however, it has been possible to obtain a preliminary reading on whether the TPS has sufficient control power to provide for both stabilization and maneuvering at high speeds. A comparison of the high-speed maneuverability of the TPS with that possessed by conventional submarines remains to be accomplished, however.

Those investigations of the dynamic behavior of the TPS, completed to date, are described in the following sections. The (1) use of linearized equations and (2) the elimination of second-order forces and moments (arising from control couplings) facilitated a limited amount of theoretical analysis. However, the bulk of the stability and control investigations, described herein, was accomplished with the aid of analog computer simulation. Representative machine runs are included.

7.2 THE LINEARIZED EQUATIONS OF MOTION

Section VI presented the dynamic equations of motion (6-1) that describe the six-degree-of-freedom response of the TPS to control forces and moments. Equations (6-1) are nonlinear for large motions, since they contain products of dependent variables as well as the trigonometric functions introduced by the Euler angle transformations. If small perturbations from trim are assumed, it is legitimate to (1) make the small-angle approximation that $\sin A = \tan A = A$ and $\cos A = 1$ and (2) neglect the products of perturbation variables. Equations (6-1) then become (for symmetrical propeller operation):

$$\begin{array}{rcl}
 m_1 \dot{u} & - \Sigma X & = X_c \\
 m_2 \dot{v} + m_1 \dot{\psi} u_0 & - \Sigma Y & = Y_c \\
 m_3 \dot{w} - m_1 \dot{\theta} u_0 & - \Sigma Z & = Z_c \\
 I_{xx} \ddot{\phi} & - \Sigma K & = K_c \\
 I_{yy} \ddot{\theta} & - \Sigma M & = M_c \\
 I_{zz} \ddot{\psi} & - \Sigma N & = N_c
 \end{array} \quad \left. \vphantom{\begin{array}{rcl} m_1 \dot{u} & - \Sigma X & = X_c \\ m_2 \dot{v} + m_1 \dot{\psi} u_0 & - \Sigma Y & = Y_c \\ m_3 \dot{w} - m_1 \dot{\theta} u_0 & - \Sigma Z & = Z_c \\ I_{xx} \ddot{\phi} & - \Sigma K & = K_c \\ I_{yy} \ddot{\theta} & - \Sigma M & = M_c \\ I_{zz} \ddot{\psi} & - \Sigma N & = N_c \end{array}} \right\} (7-1)$$

Note that the forward-velocity disturbance variable, \bar{u} , does not enter into the last five equations of (7-1). The latter, therefore, define the response of a five-degree-of-freedom system in which the forward velocity, u_0 , remains constant.

If we introduce the transformation

$$\dot{z} = -u_0 \sin \theta + \bar{w} \cos \theta$$

where \dot{z} is the vertical velocity of the submarine relative to an earth coordinate system and then make use of the small-angle assumptions, there is obtained

$$\dot{z} = -u_0 \theta + \bar{w} \quad (7-2)$$

Substituting Equations (5-0) and Equation (7-2) into the last five equations of (7-1) yields:

$$\left. \begin{aligned} Y: & \quad m_2 \ddot{\bar{v}} - Y_v \bar{v} + (m_1 u_0 - Y_r) \dot{\psi} - Y_p \dot{\phi} & = Y_c \\ Z: & \quad m_3 \ddot{z} - Z_w \dot{z} + [(m_3 - m_1) u_0 - Z_g] \dot{\theta} - Z_w u_0 \theta & = Z_c \\ K: & \quad I_{xx} \ddot{\phi} - K_p \dot{\phi} - M_\theta \phi - K_v \bar{v} - K_r \dot{\psi} & = K_c \\ M: & \quad I_{yy} \ddot{\theta} - M_g \dot{\theta} - [M_w u_0 + M_\theta] \theta - M_w \dot{z} - M_r \dot{\psi} & = M_c \\ N: & \quad I_{zz} \ddot{\psi} - N_r \dot{\psi} - N_v \bar{v} - N_p \dot{\phi} - N_g \dot{\theta} & = N_c \end{aligned} \right\} (7-3)$$

The control forces and moments appear on the right hand side of Equations (7-3), and have been defined earlier by Equation (5-15). If the nonlinear, control-coupling terms are not significant in the operating regime, Equations (7-3) become a set of linear differential equations and the dynamic behavior of the TPS can be investigated using methods of operational calculus. Note that examination of the depth-changing behavior has been facilitated by transforming the body-axis variable, \bar{w} , to the earth-referenced variable, \dot{z} .

7.3 ANALYTICAL STUDIES

A brief analytical investigation of the simplified pitch/yaw dynamics of the TPS was undertaken as a first step towards accomplishing the stability and control work outlined above. Recognizing that this was to be followed by a more complete examination of submarine dynamics via computer simulation the objectives of the study were limited to (a) obtaining an understanding of the basic uncontrolled* behavior of the TPS, and (b) outlining the control system requirements for pitch, depth and course control of the vehicle.

The uncontrolled pitch-plane dynamics of the submarine can be described approximately by the M and Z equations of the set (7-3). Focusing attention on the response to applied pitching moment and describing this pitching moment simply by $M_S \delta_M$ the following transfer function results: (S is the Laplace operator)

$$\frac{\theta(s)}{\delta_M} = \frac{M_S (s m_3 - z_w)}{s^3 (m_3 I_{yy}) + s^2 (-m_3 M_y - z_w I_{yy}) + s (-m_3 M_\theta + z_w M_y - M_w m_1 u_0 - M_w z_g) + z_w M_\theta} \quad (7-4)$$

In a similar manner, the simplified yaw response to a yaw moment $N_S \delta_N$ can be obtained from the Y and N equations of the set (7-3). It is:

$$\frac{\dot{\psi}}{\delta_N}(s) = \frac{-N_S (m_2 s - Y_r)}{s^2 (m_2 I_{zz}) - s (m_2 N_r + I_{zz} Y_r) + N_r Y_r + N_r (m_1 u_0 - Y_r)} \quad (7-5)$$

If one now substitutes the numerical values of the physical constants and stability derivatives indicated, each of the resulting characteristic determinants (i. e. the denominators) of (7-4) and (7-5) will prove to possess a negative coefficient. Thus, the uncontrolled submarine is unstable in both pitch and yaw. Mathematically, this instability arises primarily from the magnitudes and signs of the angle-of-attack/sideslip derivatives M_w and N_r .

* The word "uncontrolled" is used to describe the dynamics of the TPS without stability augmentation through automatic control.

but is also due to other dynamic effects. Physically, it arises from the fact that if θ or ψ are disturbed, a hydrodynamic upsetting moment rather than a righting moment, is developed.

Accordingly, the functions of any automatic control system designed for the TPS should be (a) to stabilize the inherently unstable vehicle, and (b) to "shape" the dynamic behavior of the vehicle to desired specifications. Taken together these two functions constitute what is often called "stability augmentation".

Based on approximations to the higher order transfer function represented by (7-4) the pitch-plane analytical investigation was carried to the point of determining crude ranges for stabilization gains for the pitch axis. Since this work formed the basis for, and was corroborated by, an analog computer study (see below) it is not described here.

In the sections to follow, stability augmentation techniques which are applicable to the multi-degree-of-freedom control problem in general are described briefly. Attention is then given to the pitch-plane dynamics (including an analog computer investigation). Finally, a few remarks are made relative to the yaw-plane dynamics.

7.4 STABILITY AUGMENTATION

Two stability augmentation techniques were investigated. In the first, called direct-axis-stabilization (and abbreviated to D. A. S. for convenience), feedback control signals are selected which are functions of those motion variables which can be identified with the instability of the vehicle or with the particular response which needs "shaping" or improvement. These signals are then used to generate control forces and moments in the same axis. For example, the term $-(M_w u_0 + M_\theta)$, which appears in the pitching moment expression (Eq. 7-3), takes on a negative value when $u_0 > M_\theta / M_w$. For the TPS this speed is about 1.7 ft/sec. Above this speed the vehicle exhibits the instability previously alluded to. In order to stabilize the pitch axis let the blade angle variable which produces pitching moment, δ_m , be defined by:

$$\delta M = \delta M_C - \bar{K}_\dot{\theta} \dot{\theta} - \bar{K}_\theta \theta \quad (7-6)$$

where δM_C is the commanded value of δM (i. e. the control-loop input), δM is the actual blade deflection(s) and $\bar{K}_\dot{\theta}$ and \bar{K}_θ are pitch-rate and pitch-angle feedback respectively. By proper choice of the gains $\bar{K}_\dot{\theta}$ and \bar{K}_θ one can modify the coefficients in the transfer function (7-4), which would then be $\frac{\theta}{\delta M_C}(s)$. The inherent instability can be removed and, within limits, the dynamic response can be shaped. This effect can be seen in another way by substituting (7-6) into the M equation of the set (7-3).

$$I_{yy}\ddot{\theta} + [M_y\bar{K}_\dot{\theta} - M_y]\dot{\theta} + [M_y\bar{K}_\theta - M_\theta - M_{w\dot{u}_0}]\theta - M_{r\dot{\psi}} - M_{w\dot{z}} = M_S\delta M_C \quad (7-7)$$

in which M_C has been simplified to include only the primary control term $M_S\delta M_C$. Although (7-7) shows how the rate and position gains $\bar{K}_\dot{\theta}$ and \bar{K}_θ augment the damping and stiffness in the M equation of the uncontrolled submarine, it does not, of course, show the complete effect of these feedbacks on the characteristic determinant of (7-4). Note also that direct-axis stabilization does not effect in any way the hydrodynamic coupling terms $M_{r\dot{\psi}}$ and $M_{w\dot{z}}$ in (7-7). Coupling terms such as these produce higher-order characteristic determinants, illustrated by (7-4).

In order to determine what benefits, if any, might accrue in reducing the order of these determinants, a second stability augmentation technique was investigated briefly. In this technique feedback signals which are generated by motion variables in one axis are used to develop control forces/moments in another axis. These feedbacks can be adjusted to effectively cancel the hydrodynamic coupling terms and for this reason the method is called decoupling stabilization. A control equation which illustrates this is:

$$\Delta m = \Delta m_c - \bar{K}_\theta \dot{\theta} - \bar{K}_\theta \theta - \bar{K}_\dot{z} \dot{z} + \bar{K}_\psi \dot{\psi} \quad (7-8)$$

which is like (7-6) except that the "decoupling feedbacks" $\bar{K}_\dot{z} \dot{z}$ and $\bar{K}_\psi \dot{\psi}$ have been added. If one now substitutes (7-8) into (7-3), as was done previously with (7-6), it can be seen that by proper choice of $\bar{K}_\dot{z}$ and \bar{K}_ψ the hydrodynamic coupling terms can be made to vanish. It will be shown later that in the case of the pitch axis, illustrated in (7-8), the direct-axis terms \bar{K}_θ and \bar{K}_θ must be retained for reasons of stability. Hence, in some of the analog computer runs to follow this technique is called decoupling-plus-direct-axis stabilization.

7.5 PITCH-PLANE DYNAMICS

The analytical studies, described briefly above, were followed by an analog computer simulation to further investigate the high-speed pitch-plane dynamics of the TPS. Motion was arbitrarily confined to the $x-z$ plane. The equations of motion, taken from (7-3) are:

$$\left. \begin{aligned} m_3 \ddot{z} - Z_w \dot{z} + [(m_3 - m_1) u_0 - Z_q] \dot{\theta} - Z_w u_0 \theta &= Z_c \\ I_{yy} \ddot{\theta} - M_q \dot{\theta} - [M_w u_0 + M_\theta] \theta - M_w \dot{z} &= M_c \\ m_1 \ddot{u} - X_u \dot{u} &= X_c \\ I_{xx} \ddot{\phi} - K_p \dot{\phi} - M_\phi \phi &= K_c \end{aligned} \right\} (7-9)$$

The X and K equations were mechanized in order to determine how the non-linear control-coupling terms contained in X_c and K_c would effect velocity and roll angle. A roll stabilization loop was used in all of the analog computer

* The single and double bars have no special significance.

runs. The roll-rate and roll-angle gains $K_{\dot{\theta}}$ and K_{θ} (see below) were arbitrarily selected to yield an undamped natural frequency of about 1.0 rad/sec and a damping ratio of 0.7 critical for the uncoupled roll dynamics.

The control equations are:

$$\begin{aligned}
 \delta z &= \delta f_c - \delta i_a c + K_{\dot{z}} \dot{z} + K_z z - K_{\dot{\theta}} \dot{\theta} - K_{\theta} \theta \\
 \delta m &= \delta f_c + \delta i_a c - K_{\dot{\theta}} \dot{\theta} - K_{\theta} \theta - K_{\dot{z}} \dot{z} \\
 \delta x &= \Delta \delta f_c + \Delta \delta a c \\
 \delta \kappa &= \Delta \delta f_c - \Delta \delta a c + K_{\dot{\theta}} \dot{\theta} + K_{\theta} \theta \\
 \delta i_a &= \frac{1}{2} (\dot{\delta m} - \delta z) \\
 \delta i_f &= \frac{1}{2} (\delta m + \delta z) \\
 \Delta \delta a &= \frac{1}{2} (\delta x - \delta \kappa) \\
 \Delta \delta f &= \frac{1}{2} (\delta x + \delta \kappa)
 \end{aligned}
 \tag{7-10}$$

Both direct-axis and decoupling gains are shown in the equations, however not all of these were used in every analog run. Note that commanded values are differentiated from actual values by the subscript C.

The control forces and moments, with motion confined to the $x-z$ plane, are given by:

$$\begin{aligned}
 X_c &= X_{\Delta S} \delta x + X_{(\Delta S)^2} \left((\Delta \delta_f)^2 + (\Delta \delta_a)^2 \right) + X_{\delta^2} (\delta_{if}^2 + \delta_{ia}^2) \\
 Z_c &= Z_S \delta z + Z_{\Delta S, S} (\Delta \delta_f \delta_{if} - \Delta \delta_a \delta_{ia}) \\
 M_c &= M_S \delta m - l_2 Z_{\Delta S, S} (\Delta \delta_f \delta_{if} + \Delta \delta_a \delta_{ia}) \\
 K_c &= K_{\Delta S} \delta k + K_{(\Delta S)^2} \left((\Delta \delta_f)^2 - (\Delta \delta_a)^2 \right) + K_{\delta^2} (\delta_{if}^2 - \delta_{ia}^2)
 \end{aligned}
 \tag{7-11}$$

7.5.1 Discussion of Analog Runs - High-Speed Case

The response of the basic submarine with all stability augmentation terms set to zero and no control coupling terms included is shown in Figure 7-1. In all of the analog computer work, runs were made with and without the nonlinear components of (7-11) and the effect of these components was found to be negligible. These terms were therefore left out of the runs reproduced in this report (except for Figure 7-6). Time histories of pitch angle, depth change, roll angle and forward velocity are shown in Figure 7-1, reading from top to bottom. The instability of the uncontrolled submarine is obvious. Notice that roll angle and forward velocity perturbations are too small to appear in the traces. In all runs, ϕ and \bar{u} were monitored and found to be negligibly small.

In Figure 7-2, feedback gains necessary to decouple the pitch and depth responses were used. The response to a δ_{mc} input (equal magnitudes of δ_{ifc} and δ_{iac}) is a divergent pitch angle, but the depth remains constant. The pitch terms in the depth equation have been effectively cancelled by the decoupling feedback. However, the system is still unstable in pitch. In this figure, and in all of the remaining analog runs, the forward and aft

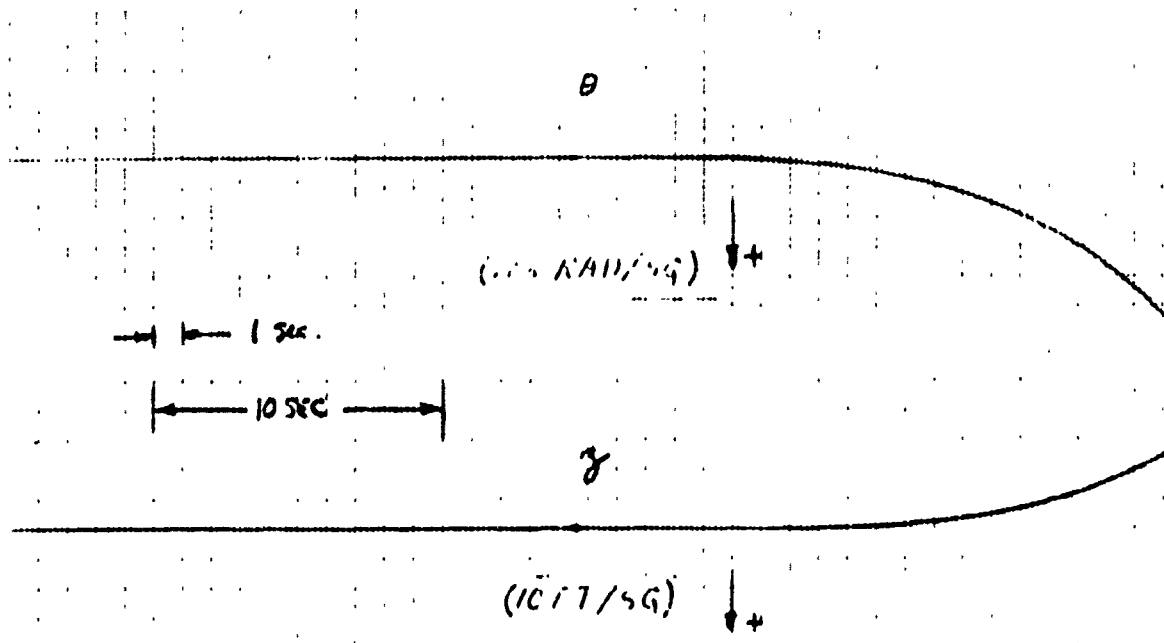


FIG 7-1
 BASIC SUBMARINE RESPONSE
 (ALL FEEDBACK GAINS ZERO)
 LINEAR SYSTEM.

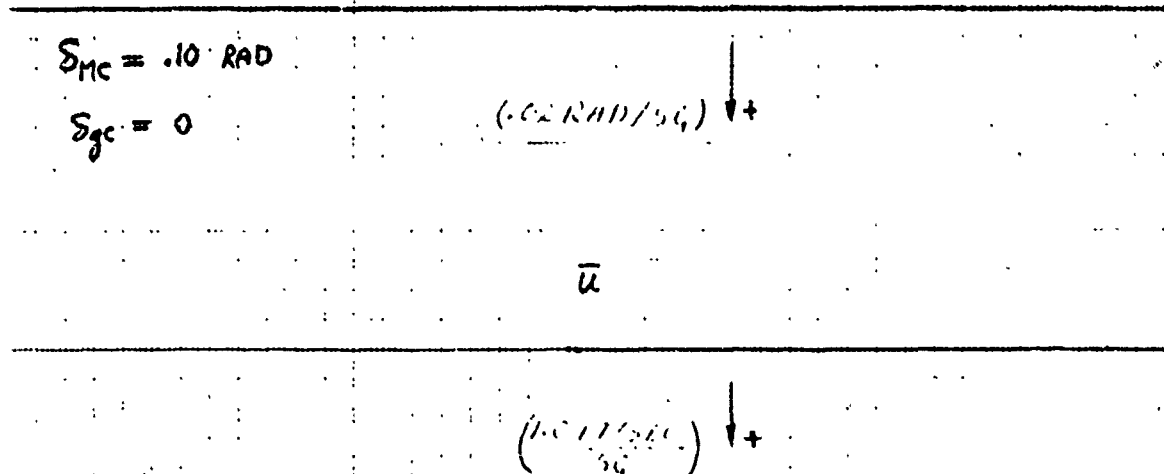


FIGURE 7-1 Basic Submarine Response
 (All Feedback Gains Zero) Linear System

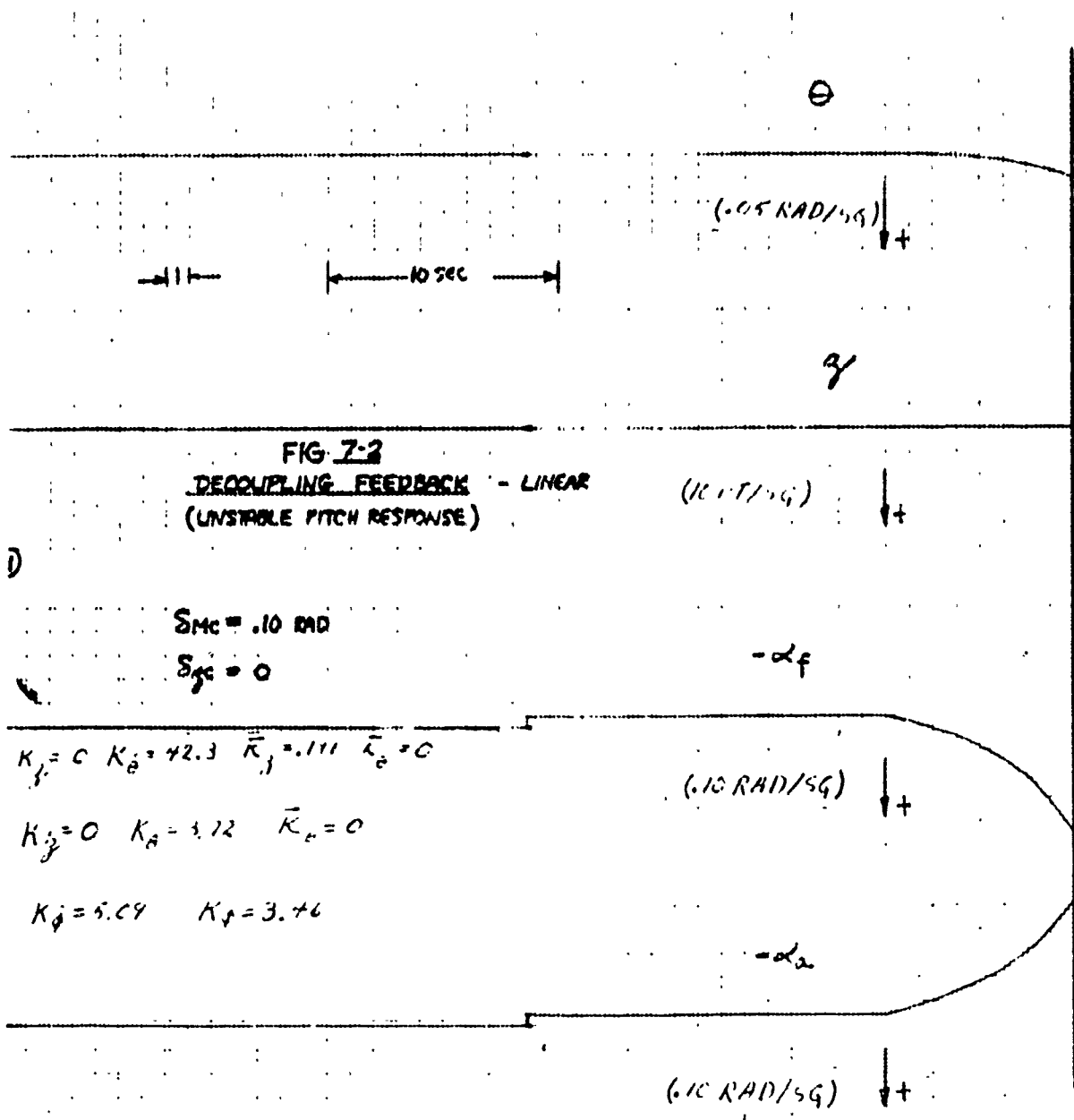


FIGURE 7-2 Decoupling Feedback - Linear (Unstable Pitch Response)

propeller angles-of-attack are traced. These are the total changes in α , over and above the trim α , called for as a result of the particular feedbacks being used.

In Figure 7-3, direct-axis feedback is added to the system of Figure 7-2. The gains were selected to shape the pitch natural frequency to 0.1 rad/sec, with 0.7 critical damping. There is no depth change because $\delta z_c = 0$. Note that the α_f needed to achieve a steady-state pitch angle of about 4° is approximately 25° . This angle may be beyond the actual stall angle-of-attack of the blades but this depends upon blade design. In any event blade angles-of-attack in excess of 20 or 25 degrees were considered undesirable for the purposes of this study.

In Figure 7-4, direct-axis pitch-rate stabilization only is used, (pitch-angle gain, $\bar{K}_\theta = 0$). The z trace of previous runs has been replaced by the \dot{z} trace. A steady pitch angle of about 9 degrees and a climb-rate of about 7 ft/sec are obtained after about 500 sec, for a $\delta \dot{\theta}_c$ step input of .05 rad. The angles-of-attack, which are at the commanded value at $t = 0$, rapidly reverse as the vehicle pitches up (the effect of the $\bar{K}_{\dot{\theta}}$ feedback) and eventually settle out to about .025 rad.

The relatively poor response shown in Figure 7-4 can be improved by adding pitch-angle feedback, \bar{K}_θ . This improvement is shown in Figure 7-5, where it is seen that the pitch and depth-rate responses reach 95% of their final values in about 80 seconds. The run of Figure 7-5 is repeated in Figure 7-6 with the nonlinear control-coupling terms of equation (7-11) included in the simulation in order to show that their effect is negligible.

The response of the TPS to a δz_c input, when direct-axis stabilization is employed, is shown in Figure 7-7. In this case, the submarine does not reach a steady-state condition where the hull angle of attack is zero (as is the case in Figures 7-5 and 7-6), unless $u_0 > \frac{-M_a + M_s \bar{K}_\theta}{M_w}$

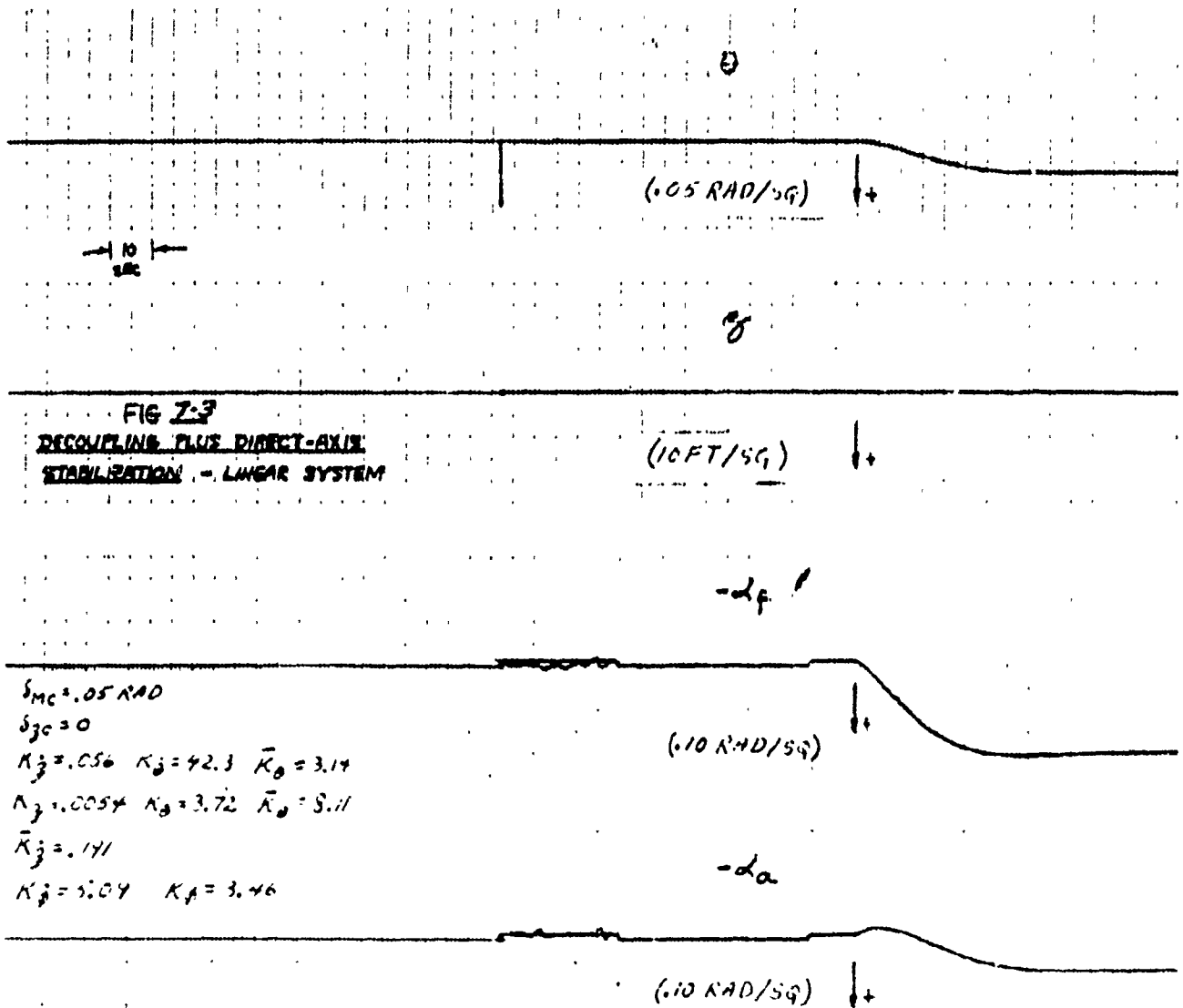


FIGURE 7-3 Decoupling Plus Direct-Axis Stabilization - Linear System.

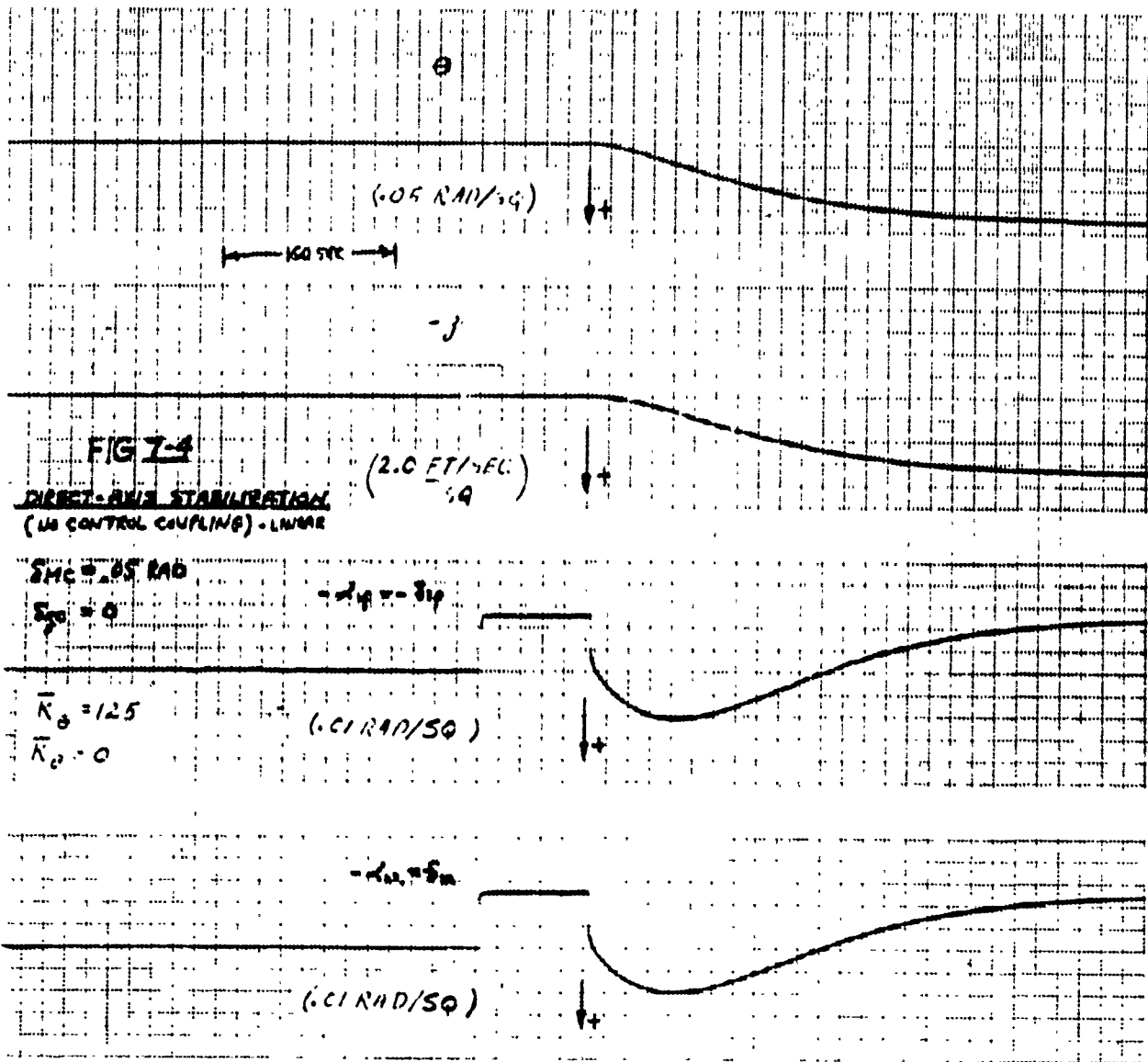


FIGURE 7-4 Direct-Axis Stabilization (No Control Coupling) - Linear

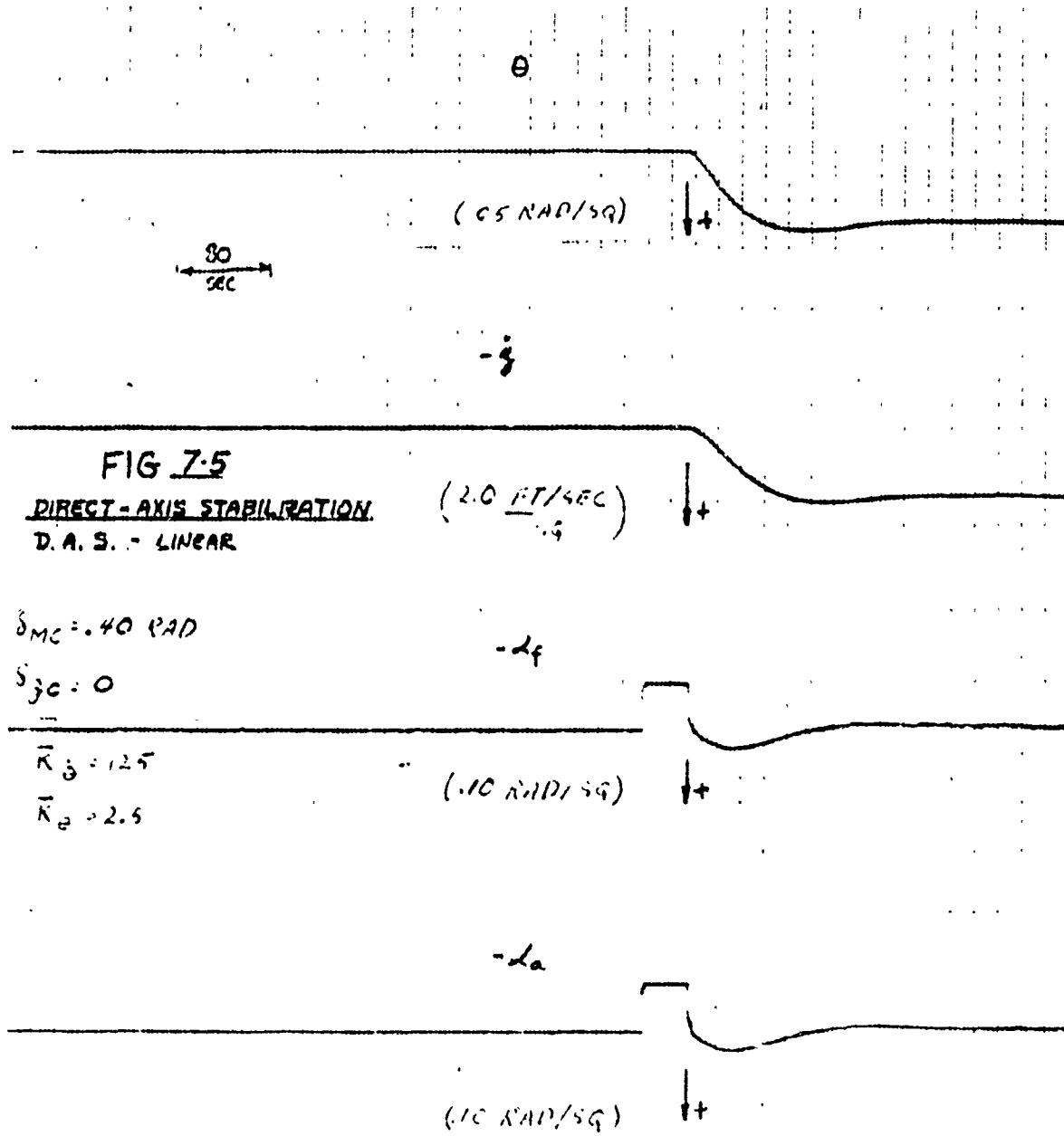


FIGURE 7-5 Direct-Axis Stabilization - Linear

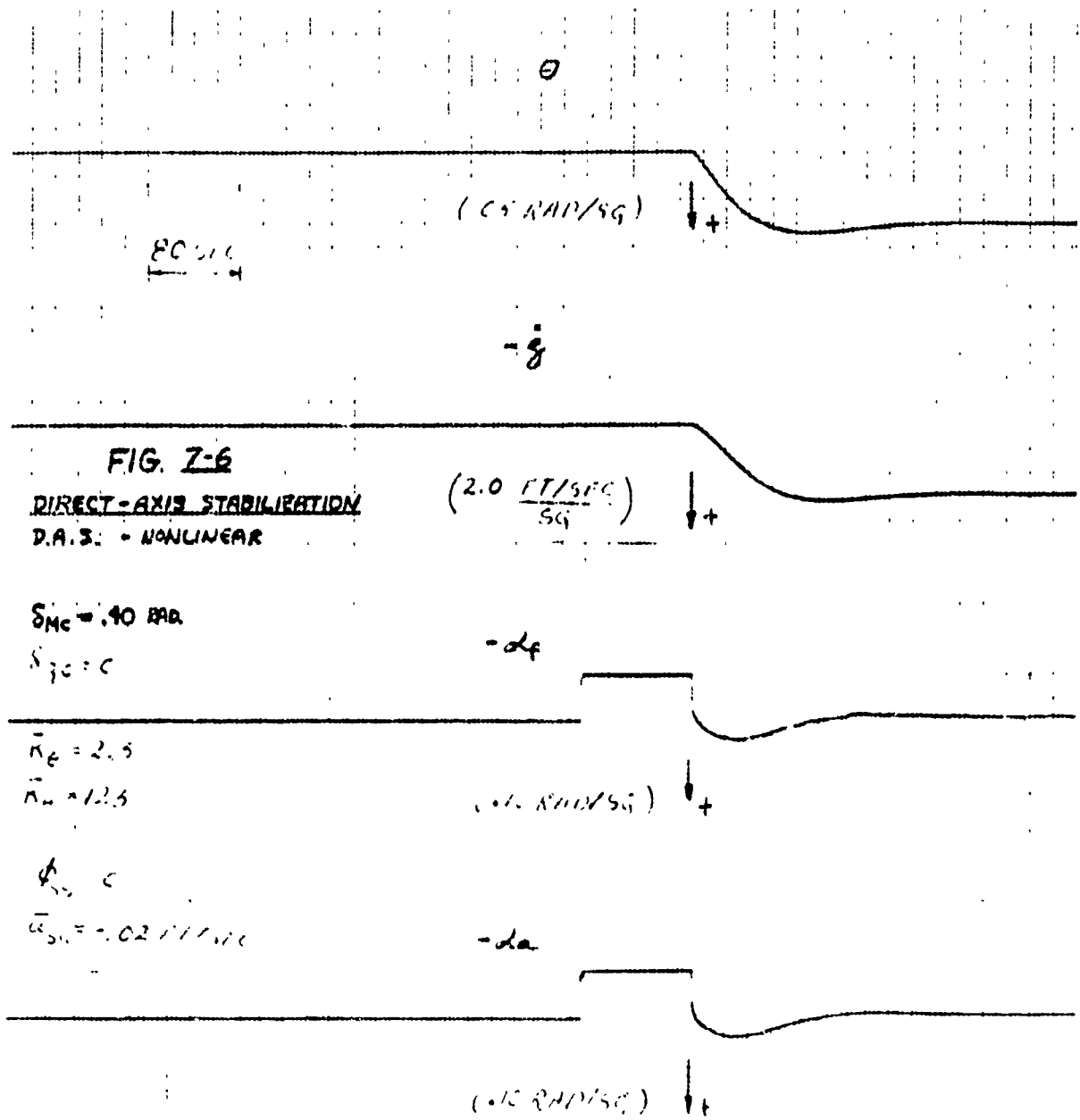


FIGURE 7-6 Direct-Axis Stabilization - Nonlinear

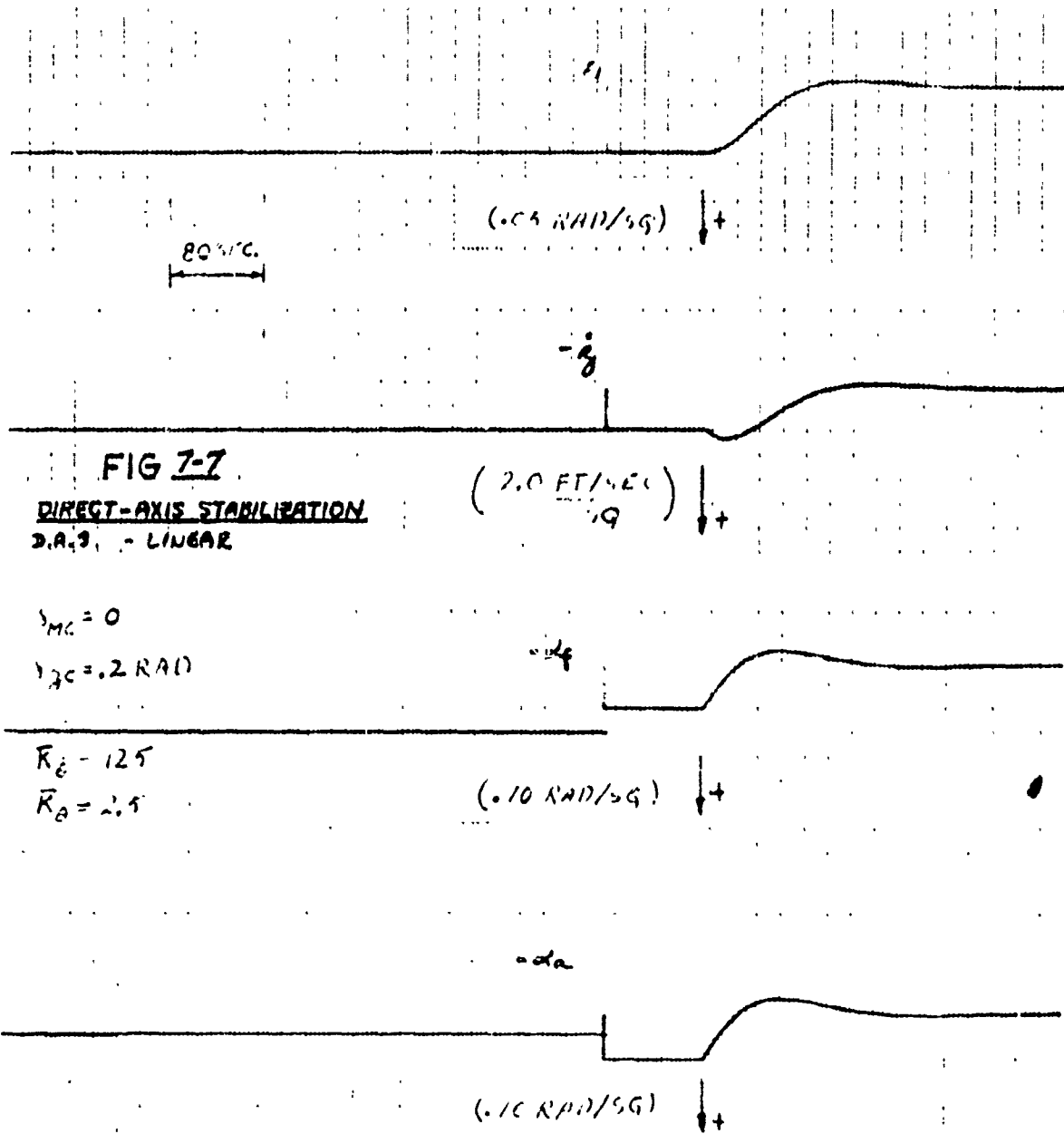


FIG 7-7
DIRECT-AXIS STABILIZATION
 D.A.S. - LINEAR

$\gamma_{MC} = 0$

$\gamma_{\beta} = 0.2 \text{ RAD}$

$R_{\beta} = 125$

$R_{\alpha} = 2.5$

FIGURE 7-7 Direct-Axis Stabilization - Linear

The response times for Figures 7-6 and 7-7 are about the same, but the steady-state α are higher and the depth-rate is lower in Figure 7-7. In other words, as should be anticipated, more efficient diving or climbing is obtained with pitching-moment input than with z -force input.

Combined direct-axis plus decoupling stabilization is explored in Figure 7-8, where a depth-rate time constant of 14.3 seconds and a pitch-angle natural frequency and damping ratio of .10 rad/sec and 0.70 respectively are employed.* The decoupling and direct-axis feedback sensitivities used result in steady-state pitch angle and depth rate responses to a step input given by the following equations:

$$\theta_{ss} = \frac{1}{\frac{-M_{\theta} - M_w u_0}{M_S} + \bar{K}_{\theta}} \delta_{mc} \quad (7-12)$$

$$\dot{z}_{ss} = \frac{1}{\frac{z_w}{z_S} + K_z} \delta_{zc} \quad (7-13)$$

In order to cause the submarine to point in the direction of its total velocity vector, both δ_{mc} and δ_{zc} command inputs must be used simultaneously. It can be shown that having $\dot{z} = -u_0 \theta$ (zero hull angle-of-attack) requires that $\delta_{zc} = 8.14 \delta_{mc}$. Note that $\delta_{xc} = .814 \delta_{mc}$ and that $\dot{z} = -40\theta$ in Figure 7-8. The blade angles-of-attack are very small and the response times are fast for this case.

Figure 7-9 indicates that responses similar to those of Figure 7-8 can be obtained by direct-axis stabilization alone and through the use of pitch-angle command inputs alone. Response times of about thirty seconds result from the gains indicated on the figure. These response times can be reduced even further by increasing the \bar{K}_{θ} feedback gain. It can be concluded from Figures 7-8 and 7-9 that either stabilization technique can be used with

* Due to the decoupling, these loops are first and second-order respectively.

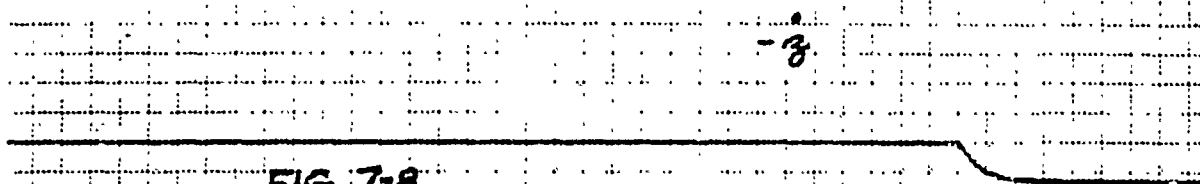
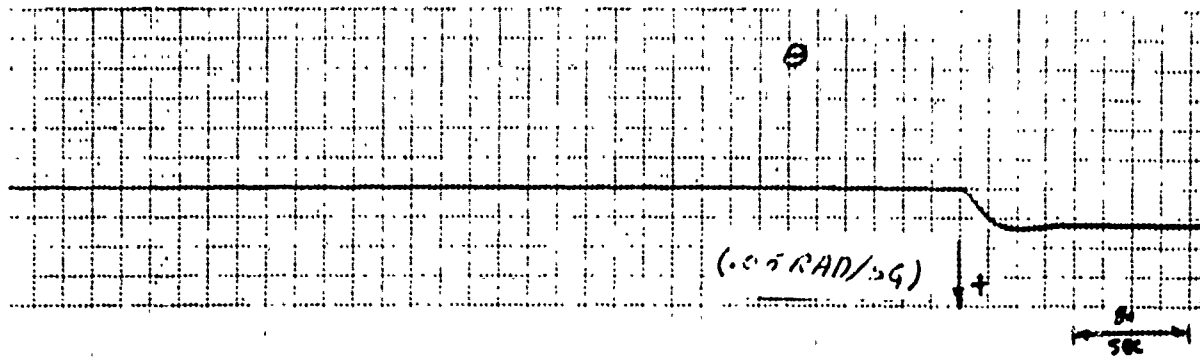
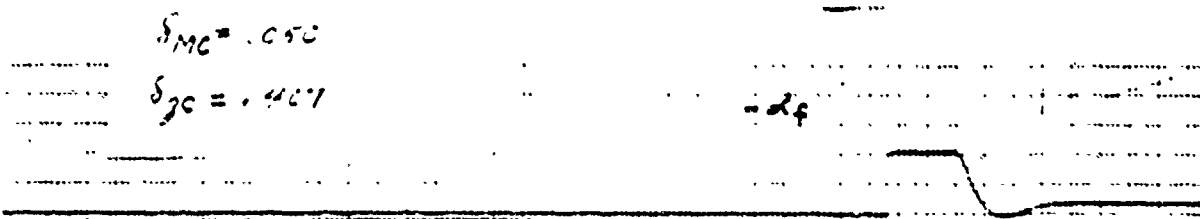


FIG 7-8

DECOUPLING + D.A. STABILIZATION-LINEAR (2 FT/SEC) ↓ +

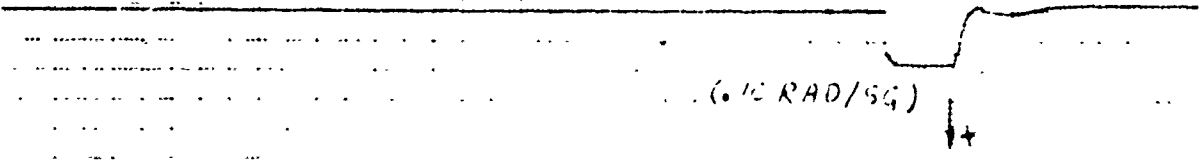


$K_j = 0$ $K_e = 3.72$ $\bar{K}_e = 8.11$
 $K_j = 0.056$ $K_i = 42.3$ $\bar{K}_i = 3.14$

(0.10 RAD/SG) ↓ +

$K_f = 3.46$ $K_f = 5.09$
 $\bar{K}_j = 1.31$

-2.4



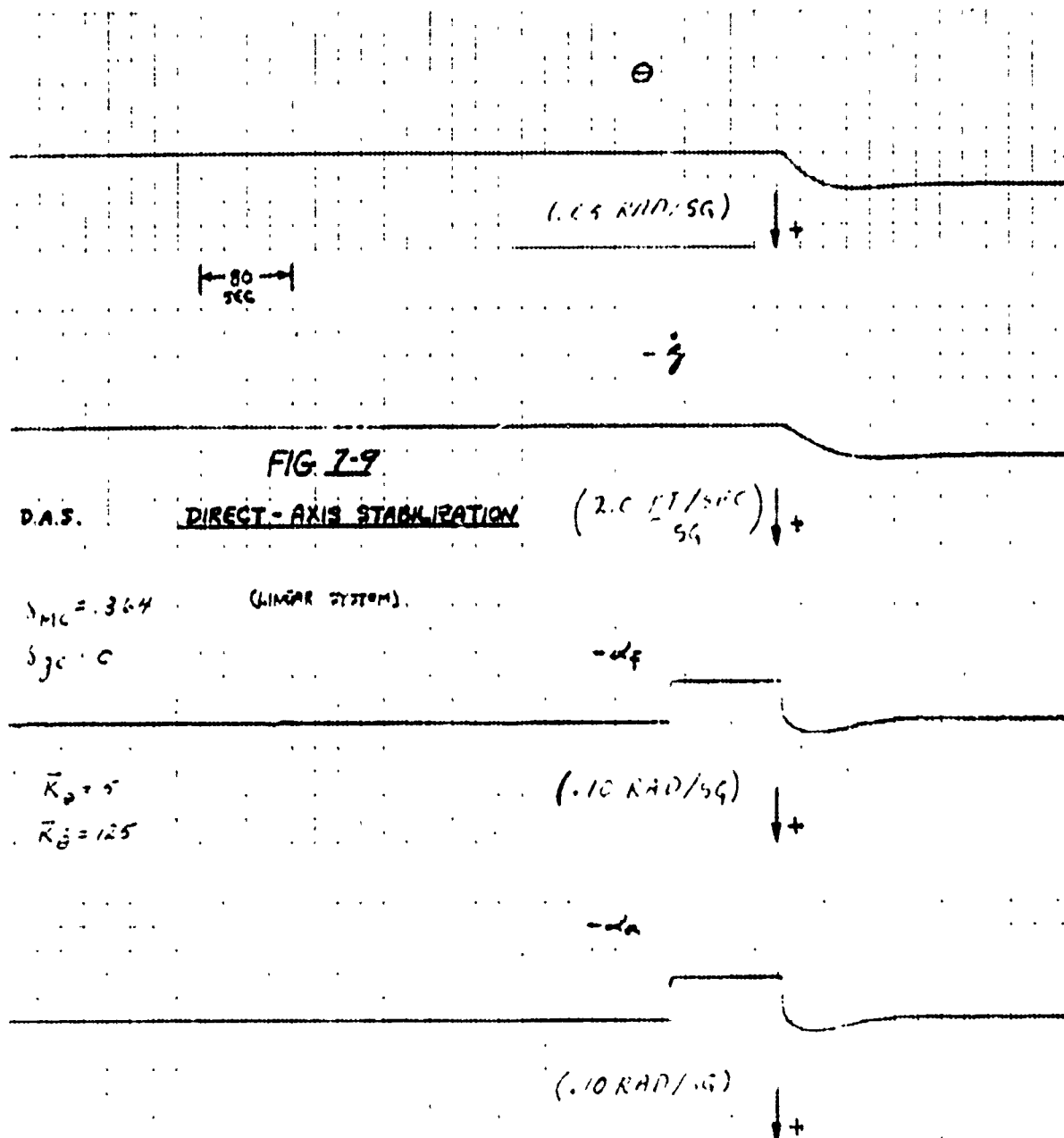


FIG. 7-9

D.A.S. DIRECT-AXIS STABILIZATION

$\lambda_{MC} = .364$ (LINEAR SYSTEM)

$\delta_{gc} = 0$

$\bar{K}_\theta = 5$
 $\bar{K}_\beta = 125$

FIGURE 7-9 Direct-Axis Stabilization

similar results in terms of pitch angle and depth rate dynamic and static responses, and that about the same "economy" in using up the useful range of blade angle-of-attack is achieved. Accordingly, there seems to be little to recommend the decoupling-stabilization technique, in the pitch-plane, when climb or dive maneuvering is involved, since a \dot{z} sensor would be needed to implement $K_{\dot{z}}$ in the δM control equation (7-10). As has been shown above, climb and dive maneuvering can be performed efficiently with direct-axis feedback and δM inputs alone. However, in the case of an attitude stabilizing and depth-keeping control system, or in the case of docking maneuvers, there may be some advantage to decoupling stabilization. This matter will be explored further in the work that remains to be done under the present contract.

7.6 YAW-PLANE DYNAMICS

At the time of writing this report the yaw-plane analog computer studies were still in progress. However, preliminary calculations have shown that the stabilization problems in the yaw plane are quite similar to those in the pitch plane. It should be possible, therefore, to achieve stable and acceptable controlled-submarine behavior, but a firm conclusion to this effect cannot be made at this time. The outcome of the analog-computer study will indicate whether or not the strong yaw-roll coupling, due to the presence of the sail, is critical in terms of the demands made upon the available control forces and moments. Thus, while it is a relatively simple matter to calculate the stabilization feedbacks needed to achieve specified yaw-roll dynamics, the question is one of whether these stabilizing signals will call for more control power than is available.

VIII REMAINING STUDIES

The work scheduled in the present program is aimed at performing or completing the following tasks:

- (1) Complete the low-speed hydrodynamic studies.
- (2) Complete the analog computer study of the high-speed yaw-plane dynamics.
- (3) Perform analog computer studies of the low-speed controlled-submarine dynamics.
- (4) Draw preliminary conclusions as to the feasibility of the tandem propeller concept based upon the hydrodynamic studies, the stability and control studies, and judgments (yet to be made) of the estimated handling qualities of a Tandem Propeller Submarine.

IX
REFERENCES

1. "Naval Architectural Aspects of Submarine Design" by E. S. Arentzen and Philip Mandel. Trans. Vol. 68, 1960 of the Society of Naval Architectural & Marine Engineers (U).
2. "Qualitative Discussion of the Hydrodynamic Properties of Tandem Propeller Systems With Cyclic Pitch Control" Netherland Ship Model Basin, February 1962 (U).
3. "Force and Pressure Distribution Measurements on Eight Fuselages" by G. Lange. NACA TM #1194, October 1941.
4. "Model Investigation of the Stability and Control Characteristics of the Preliminary Design of the SSGN (FBM)" by D. B. Young, David Taylor Model Basin, Report #C-928, July 1958.
5. "A Method for Calculation of Hydrodynamic Lift for Submerged and Planing Rectangular Lifting Surfaces" by K. L. Wadlin and K. W. Christopher. NASA TR-R-14, 1959.

6. "The Stability Derivatives of an Aircrew" by H. Glauert, Royal Aircraft Establishment R & M #642, 1919 (U).
7. "Aerodynamics of the Airplane" (book) C. B. Millikan, John Wiley & Son 1941.
8. "Airfoil and Airscrew Theory" (reprint) by H. Glauert, Cambridge University Press 1943.
9. "Large Hub to Diameter Ratio Propeller With Programmed Blade Control" Netherlands Ship Model Basin, January 1962.
10. "Feasibility Study, Tandem Propeller Propulsion System for a Submarine, Electrical Machinery Specification, Revision C" U413-61-192, December 19, 1961. (U).

APPENDIX
THE LINEARIZED, LOW-SPEED, HYDRODYNAMIC FORCES
AND MOMENTS ARISING FROM THE PROPELLERS OF THE TPS

The force and moment equations resulting from the analysis described in Section 5.2.2.2 are presented in this appendix. The equations, as shown, are valid for the forward propeller only when this propeller is producing a positive thrust. Modifications in the sign of various terms are required to make the equations valid for the aft counterclockwise rotating propeller and to further handle those situations where the submarine axial motion, u , is opposite to the direction of the propeller-induced inflow velocity, U_p . It should be noted that the equations are based on body axis, and that all terms involving $(v + r l_2)$ and $(w - q l_2)$ have been multiplied by 2 to account for the cross-flow velocity distribution around the hull.

$$\begin{aligned}
 x]_f &= \frac{NPA}{2} R^2 \Omega^2 \left\{ C_{Lx} \left[\epsilon_0 \left(1 + 2 \frac{p}{\Omega} \right) - \frac{u + \xi i}{R \Omega} + 2a_1 \frac{w - q k_2}{R \Omega} - 2b_1 \frac{u + \xi i}{R \Omega} \right. \right. \\
 &\quad \left. \left. - C_{D_0} \left(\frac{u + \xi i}{R \Omega} \right) \right. \right. \\
 &\quad \left. \left. - f_1 C_{Lx}^2 \left[\epsilon_0 \left(\epsilon_0 \frac{u + \xi i}{R \Omega} - a_1 \frac{u}{\Omega} + b_1 \frac{q}{\Omega} \right) + \left(\frac{u + \xi i}{R \Omega} \right)^2 \frac{a_1 + b_1}{2} \right] \right\}
 \end{aligned}$$

$$\begin{aligned}
 y]_f &= \frac{NPA}{2} R^2 \Omega^2 \left\{ -\frac{C_{Lx}}{2} \left[\epsilon_0 \frac{q}{\Omega} + b_1 \frac{u + \xi i}{R \Omega} \right] \right. \\
 &\quad \left. + 2C_{D_0} \left(\frac{v + k_1 k_2}{R \Omega} \right) \right. \\
 &\quad \left. - f_1 C_{Lx}^2 \left[\epsilon_0 \left(-2\epsilon_0 \frac{v + k_1 k_2}{R \Omega} - \frac{q}{\Omega} + b_1 + 2b_1 \frac{p}{\Omega} \right) \right. \right. \\
 &\quad \left. \left. + a_1 \left(b_1 \frac{v - q k_2}{R \Omega} - \frac{a_1}{2} \frac{v + k_1 k_2}{R \Omega} \right) \right. \right. \\
 &\quad \left. \left. - b_1 \left(\frac{u + \xi i}{R \Omega} + \frac{3b_1}{2} \frac{v + k_1 k_2}{R \Omega} \right) \right] \right\}
 \end{aligned}$$

$$\begin{aligned}
 z]_f &= \frac{NPA}{2} R^2 \Omega^2 \left\{ -\frac{C_{Lx}}{2} \left[\epsilon_0 \frac{k}{\Omega} - a_1 \frac{u + \xi i}{R \Omega} \right] \right. \\
 &\quad \left. + 2C_{D_0} \left(\frac{w - q k_2}{R \Omega} \right) \right. \\
 &\quad \left. + f_1 C_{Lx}^2 \left[\epsilon_0 \left(\frac{k}{\Omega} + 2\epsilon_0 \frac{w - q k_2}{R \Omega} + a_1 + 2a_1 \frac{p}{\Omega} \right) \right. \right. \\
 &\quad \left. \left. + a_1 \left(-\frac{u + \xi i}{R \Omega} - b_1 \frac{v + k_1 k_2}{R \Omega} + \frac{3a_1}{2} \frac{w - q k_2}{R \Omega} \right) \right. \right. \\
 &\quad \left. \left. + \frac{b_1^2}{2} \frac{w - q k_2}{R \Omega} \right] \right\}
 \end{aligned}$$

$$\begin{aligned}
 K]_f &= \frac{NPA}{2} R^3 \Omega^2 \left\{ C_{1c} \left[\epsilon_0 \frac{u+5i}{R\Omega} - \frac{a_1}{2} \frac{k}{\Omega} + \frac{b_1}{2} \frac{q}{\Omega} \right] \right. \\
 &\quad + C_D \left(1 + 2 \frac{P}{\Omega} \right) \\
 &\quad + f C_{1c}^2 \left[\epsilon_0^2 \left(1 + 2 \frac{P}{\Omega} \right) + \epsilon_0 \left(-2 \frac{u+5i}{R\Omega} + 2a_1 \frac{w-9k_2}{R\Omega} \right. \right. \\
 &\quad \quad \left. \left. - 2b_1 \frac{v+k_2}{R\Omega} \right) \right. \\
 &\quad \quad + a_1^2 \left(\frac{1}{2} + \frac{P}{\Omega} \right) + a_1 \frac{k}{\Omega} \\
 &\quad \quad \left. \left. + b_1^2 \left(\frac{1}{2} + \frac{P}{\Omega} \right) - b_1 \frac{q}{\Omega} \right] \right\}
 \end{aligned}$$

$$\begin{aligned}
 M]_f &= \frac{NPA}{2} R^2 \Omega^2 \left\{ C_{1c} \left[\frac{b_1}{2} \left(-\epsilon_0 \frac{k}{\Omega} + a_1 \frac{u+5i}{R\Omega} \right) \right. \right. \\
 &\quad \left. \left. + R \left(-2\epsilon_0 \frac{v+k_2}{R\Omega} + \frac{b_1}{2} + a_1 \frac{P}{\Omega} - \frac{q}{2\Omega} \right) \right] \right. \\
 &\quad + C_D \left[2b_1 \frac{w-9k_2}{R\Omega} - \frac{R}{2} \frac{q}{\Omega} \right] \\
 &\quad + f C_{1c}^2 \left[\epsilon_0^2 \left(2\epsilon_0 \frac{w-9k_2}{R\Omega} + \frac{k}{\Omega} + 2 + 2a_1 \frac{P}{\Omega} \right) \right. \\
 &\quad \quad + \epsilon_0 P \left(\frac{\epsilon_0}{2} \frac{q}{\Omega} + b_1 \frac{u+5i}{R\Omega} \right) \\
 &\quad \quad + a_1 P \left(\frac{-u+5i}{R\Omega} - \frac{v+k_2}{R\Omega} b_1 + \frac{3a_1}{2} \frac{w-9k_2}{R\Omega} \right) \\
 &\quad \quad - a_1 R \left(\frac{-a_1}{8} \frac{q}{\Omega} + \frac{b_1}{4} \frac{k}{\Omega} \right) \\
 &\quad \quad \left. \left. + b_1^2 \left(\frac{k_2}{2} \frac{w-9k_2}{R\Omega} + \frac{3R}{8} \frac{q}{\Omega} \right) \right] \right\}
 \end{aligned}$$

$$\begin{aligned}
N_f = \frac{NPA}{2} R^2 \Omega^2 \left\{ C_x \left[\frac{l_2}{2} \left(-\frac{\epsilon_0 q}{R} - b_1 \frac{u + \epsilon_0 k}{R \Omega} \right) \right. \right. \\
+ R \left(2\epsilon_0 \frac{w - q l_2}{R \Omega} + \frac{1}{2} \frac{k}{\Omega} + \frac{a_1}{2} + a_1 \frac{k}{\Omega} \right) \\
+ C_0 \left[2 l_2 \frac{v + k l_2}{R \Omega} + \frac{p}{2} \frac{k}{\Omega} \right] \\
+ C_x^2 \left[\epsilon_0 l_2 \left(-2\epsilon_0 \frac{v + k l_2}{R \Omega} - \frac{q}{\Omega} + b_1 + 2 b_1 \frac{k}{\Omega} \right) \right. \\
+ \epsilon_0 R \left(a_1 \frac{u + \epsilon_0 k}{R \Omega} - \frac{\epsilon_0}{2} \frac{k}{\Omega} \right) \\
+ a_1 l_2 \left(b_1 \frac{w - q l_2}{R \Omega} - \frac{a_1}{2} \frac{v + k l_2}{R \Omega} \right) \\
+ a_1 R \left(-a_1 \frac{3}{8} \frac{k}{\Omega} + \frac{b_1}{4} \frac{q}{\Omega} \right) \\
+ b_1 l_2 \left(-\frac{u + \epsilon_0 k}{R \Omega} - \frac{3 b_1}{2} \frac{v + k l_2}{R \Omega} \right) \\
\left. \left. + b_1 R \left(-\frac{b_1}{2} \frac{k}{\Omega} \right) \right] \right\}
\end{aligned}$$